- 1 Rising atmospheric CO<sub>2</sub> concentrations: the overlooked factor promoting SW Iberian
- 2 Forest development across the LGM and the last deglaciation?

- 4 Gomes, Sandra.D.a,b,c\*
- 5 Fletcher, William.J.a
- 6 Stone, Abia
- 7 Rodrigues, Teresa<sup>b,c</sup>
- 8 Rebotim, Andreia<sup>b,c</sup>
- 9 Oliveira, Dulce b,c
- 10 Sánchez Goñi, Maria. F. d,e
- 11 Abrantes, Fatimab,c
- 12 Naughton, Filipab,c

13

- <sup>a</sup>Quaternary Environments and Geoarchaeology, Department of Geography, School of
- 15 Environment, Education and Development, The University of Manchester, Manchester, Oxford
- 16 Road, Manchester, M13 9PL, United Kingdom;
- 17 bDivisão de Geologia e Georecursos Marinhos, Instituto Português do Mar e da Atmosfera
- 18 (IPMA), Rua Alfredo Magalhães Ramalho 6, 1495-006 Lisboa, Portugal;
- 19 °Centro de Ciências do Mar do Algarve (CCMAR/CIMAR LA), Campus de Gambelas,
- 20 Universidade do Algarve, 8005-139 Faro, Portugal;
- <sup>d</sup> École Pratique des Hautes Études, EPHE, PSL Université, Paris, France;
- <sup>e</sup>Environnements et Paléoenvironnements Océaniques et Continentaux, UMR 5805,
- 23 Université de Bordeaux, Pessac, France.

24 25

- \*Corresponding author: E-mail: sandra.domingues@manchester.ac.uk (Sandra Domingues
- 27 Gomes); Address: Quaternary Environments and Geoarchaeology, Department of
- 28 Geography, School of Environment, Education and Development, The University of
- 29 Manchester, Manchester, Oxford Road, Manchester, M13 9PL, United Kingdom

- Abstract:
- 32 Across the last deglaciation, the atmospheric partial pressure of carbon dioxide (pCO<sub>2</sub>)
- increased substantially from ~180 to ~280 ppm, yet its impact on vegetation dynamics across
- this major climatic transition remains insufficiently understood. In particular, Iberian pollen
- records reveal an intriguing feature that can be related to an often overlooked role of pCO<sub>2</sub> in
- 36 shaping vegetation responses during the last deglaciation. These records reveal the near
- 37 disappearance of forests during the cold Last Glacial Maximum (LGM) and Heinrich Stadial 1
- 38 (HS1) phases and an unexpected recovery during the Younger Dryas (YD) cold phase when
- 39 pCO<sub>2</sub> increased. Here, we present high-resolution tracers of terrestrial (pollen, C<sub>29</sub>:C<sub>31</sub> organic
- biomarker) and marine (alkenone-derived Sea Surface Temperature, C<sub>37:4</sub>%, and long-chain

n-alkanes ratios) conditions from the southwestern (SW) Iberian margin Integrated Ocean Drilling Program Site U1385 ("Shackleton site") for the last 22 cal. kyra BP. This direct landsea comparison approach allows us to investigate how the Iberian Peninsula vegetation responded to major global pCO<sub>2</sub> changes during the last deglaciation.

Our results show that cool and moderately humid conditions of the LGM supported a grassland-heathland mosaic ecosystem, but low pCO<sub>2</sub> likely caused physiological drought and suppressed forest development. HS1, the coldest and most arid period, combined with sustained low pCO<sub>2</sub> values almost suppresseds forest growth in favour of Mediterranean steppe. In contrast, the warmer Bølling-Allerød, characterised by a temperature optimum and variable but generally wetter conditions, along with the rising of pCO<sub>2</sub> above 225 ppm at ~15 cal\_kyra BP, contributed to substantial forest development. During the YD, sufficient moisture combined with increasing pCO<sub>2</sub> enabledallowed—the persistencepersistance of a mixed grassland-forest mosaic despite cooler temperatures. Our study suggests that during cool and humidlow pCO<sub>2</sub> periods (LGM and YD) and HS1), the role of different pCO<sub>2</sub> values lead to contrastingenvalues—shapen—SW Iberian vegetation responses dynamics—was more pronounced compared to periods of higher pCO<sub>2</sub>. In contrast, during periods of relatively high pCO<sub>2</sub>, tTemperature and precipitation changes during periods of relatively high pCO<sub>2</sub> played the main role in shaping the distribution and composition of the vegetation.

5960 Keywords:

45

46

47 48

49

50

51

52 53

54

55

56 57

58

63

64

65

66

67

68 69

70

71

72 73

74 75

76 77

78

79

80

81

82 83

84

85 86

61 Iberian margin; Deglaciation; Last Glacial Maximum; Direct land-sea comparison; Climatic

parameters vs pCO<sub>2</sub>; Forest development; Pollen analysis

#### 1. Introduction

The last deglaciation, spanning 20-19 cal. kyra BP (e.g. Denton et al., 1981; Toucanne et al., 2008; Denton, 2010) to ~7 cal. kayr BP (e.g. Dyke and Prest, 1987; Carlson et al., 2008) was marked by a global annual mean surface air temperature increase of 5°C °a global mean temperature increase of ~5°C, depending on latitude (Annan et al., 2022) Bard et al., 1987; Alley and Clark, 1999; Clark et al., 2012), driving during progressive melting of Northern Hemisphere glaciers. This interval was interrupted by an alternation of cold and warm phases: the warmer Bølling-Allerød (BA, 15-12.5 cal. kyra BP) was bracketed by two major cold phases, the Heinrich Stadial 1 (HS1, 18.5-15 cal\_kyra BP) and the Younger Dryas (YD, 12.9 - 11.6 cal\_kayr BP), particularly in the North Atlantic region. This period was also characterized by an increase in atmospheric carbon dioxide (pCO<sub>2</sub>) concentrations (pCO<sub>2</sub>) from ~180 to ~280 ppmv (Monnin et al., 2001; Shakun et al., 2012; Marcott et al., 2014), one of the largest shifts of the last 800,000 years (Lüthi et al., 2008). This rise was not gradual, rather there were three main rapid (<200 years) pCO<sub>2</sub> rises, of ~10 to 15 ppmv, at the end of HS1, within the BA and at the onset of the YD, as recorded in the West Antarctic Ice Sheet Divide ice core (Marcott et al., 2014). Based on a direct comparison between terrestrial and marine climatic indicators from the SW Iberian margin sedimentary sequences, several works focused on the mechanisms underlying the regional atmospheric and oceanic responses to the last deglaciation (Boessenkool et al., 2001; Turon et al., 2003; Chabaud et al., 2014; Oliveira et al., 2018; Naughton et al., 2019; Cutmore et al., 2021). However, few of these records span the entire deglaciation, or offer resolution or chronological precision to detect short-term vegetation and climate shifts in detail. The high temporal resolution and robust chronology of IODP Site U1385, provide a valuable opportunity to evaluate vegetation response to climate and pCO2 changes in SW Iberia during this transitional period.

The role of pCO<sub>2</sub> throughout time as a climate driver remains intensely debated. Studies suggest the pCO<sub>2</sub> acted as (1) a primary driver of the climatic changes, leading to temperature changes in the Northern Hemisphere (Shakun et al., 2012; Marcott et al., 2014); (2) a climate amplifier, reinforcing warming that began through other processes (Alley and Clark, 1999; Clark et al., 2012); or (3) as a consequence of climate change, responding to temperature shifts rather than causing them (Denton et al., 2010).

Beyond its role in shaping global climate, pCO<sub>2</sub> directly influences plant physiology and the nature of how vegetation respondses to environmental change. The annual atmosphericbiospheric\_exchange of pCO2\_from\_\_between the atmosphere and biosphere due to photosynthetic activity iscorresponds to more than one-third of the total pCO<sub>2</sub>-stored in the atmosphere (Farquhar and Lloyd, 1993). ADuring photosynthesis, atmospheric pCO<sub>2</sub> plays a critical role in plant physiology; plants absorb pCO<sub>2</sub> through their stomata (, which are small leaf pores), and loseing water. At lower pCO<sub>2</sub>, such as during glacial periods, plants must open these pores wider or increase their number to capture enough pCO<sub>2</sub> (Royer et al., 2001). which . While this whilst enhancinges gas exchange, it also increases leads to greater water loss through transpiration, reducing water-use efficiency (WUE) and, inducing physiological drought stress, even under moderate climatic conditions (Street-Perrot et al., 1997; Körner, 2000). These effects are especially pronounced in semi-arid environments., where water limitation already constrains plant growth. PThis plasticity in stomatal conductance and density frequency is considered an adaptive trait that evolved under declining Cenozoic CO<sub>2</sub> levels, enabling plants to sustain carbon uptake as concentrations approached glacial minima (~180-190 ppmv), though at the cost of greater water loss (Wagner et al., 1997). These effects are especially pronounced in semi-arid environments. Under low pCO<sub>2</sub> conditions, species better adapted to drought and nutrient stress - —such as those typical of steppes - —are more likely to dominate, and are typically observed in colder periods. Conversely, higher pCO<sub>2</sub> levels promotes forest expansion and higher plant productivity, particularly in trees that benefit from improved WUE (Huang et al., 2007; Randall et al., 2013). However, the response to pCO<sub>2</sub> is not globally uniform, with differences in water and nutrient availability, alongside other environmental constraints, mediating the response (e.g. Tognetti et al., 2008).-

While many reconstructions of past vegetation focus only on temperature and precipitation, the importance of pCO<sub>2</sub> as a limiting factor in plant productivity, coverage, and WUE is now widely supported by both empirical and model-based studies (e.g. Cowling and Sykes, 1999; Harrison and Prentice, 2003; Claussen et al., 2013; Piao et al., 2020). Variations in pCO<sub>2</sub> not only affect plant physiological function but can also influence the composition and structure of vegetation communities. Under low pCO<sub>2</sub> conditions, species better adapted to drought and nutrient stress—such as those typical of steppes—are more likely to dominate, and typically are observed in colder periods. Conversely, higher pCO<sub>2</sub> levels promote forest expansion and higher plant productivity, particularly in trees that benefit from improved WUE (Huang et al., 2007; Randall et al., 2013). However, the response to CO<sub>2</sub> is not globally uniform. Regional differences in water and nutrient availability, along with other environmental constraints, mediate how vegetation responds to pCO<sub>2</sub> shifts (e.g. Tognetti et al., 2008). The BIOME4 model and a biome-scale reconstruction compiled from pollen records

covering the last 40,000 kyr across the Northern Hemisphere (> 30°N) reveal a level of

132 unexplained variability in vegetation patterns across both space and time (Cao et al., 2019), 133 and provide key insights into other factors than temperature, precipitation and potential 134 evapotranspiration that drive changes in vegetation dynamics and composition, such as pCO<sub>2</sub> (Ludwig et al., 2018; Cao et al., 2019). Similarly, Recent coupled vegetation-climate modelling 135 and multiproxy reconstructions have demonstrated that pCO<sub>2</sub> significantly impacts regional 136 vegetation extent and productivity across glacial-interglacial transitions (Wu et al., 2007; Wei 137 138 et al., 2021; Koutsodendris et al., 2023; Clément et al., 2024). These findings underscore the 139 need to include pCO<sub>2</sub> changes when interpreting pollen data or evaluating biome shifts 140 (Prentice et al., 2017; Cao et al., 2019). While the current-day pCO<sub>2</sub> fertilization has receiveds 141 considerable attention (e.g. Piao et al., 2020), studyingies focusing on the effects of low pCO<sub>2</sub> , and major on vegetation, or major transitions from low to high pCO<sub>2</sub>, are equally critical. 142 143 Last deglaciation vegetation changes have been widely studied across the Iberian Peninsula 144 from palaeoecological records (e.g. Peyron et al., 1998; Carrión et al., 2002; Chabaud et al., 145 2014; Combourieu Nebout et al., 2009; Dormoy et al., 2009; Fletcher et al., 2010a; Arranbari et al., 2014; Bartlein et al., 2011; Naughton et al., 2011; 2019; Tarroso et al., 2016) and, 146 147 alongside ecological niche modeling (Casas-Gallego et al., 2025), are traditionally interpreted 148 as a result of the combined effects of temperature, precipitation and evaporation changes. 149 However, q 150 Growing evidence shows that many climate reconstructions for glacial periods based on 151 vegetation records may be biased as they neglect the influence of low pCO2 on WUE. Neglecting this influence may contribute to the underestimation of past precipitation under full 152 glacial conditions (Jolly and Haxeltine, 1997; Cowling and Skyes, 1999; Gerhart and Ward, 153 2010; Prentice et al., 2017; Cleator et al., 2020; Izumi and Bartlein, 2016; Chevalier et al., 154 155 2021), a concern still highlighted by recent studies (e.g. Wei et al., 2021; Prentice et al., 2022). 156 To address pCO<sub>2</sub> related biases, inverse modelling studies to account for CO<sub>2</sub> correction have 157 been evolving for a while (e.g. Guiot et al., 2000; 2007; Wu et al., 2007; Izumi and Bartlein, 158 2016) and compared with reconstructions using Modern Analogue Techniques (Davis et al., 159 2024). However, the inverse modelling approach has some limitations relating to low 160 taxonomic resolution and dependence on the vegetation model that is not always comparable 161 with pollen assemblages (Chevalier et al., 2020; Prentice et al., 2022). Recently, Qquantitative reconstructions using methods like Tolerance Weighted Averaging Partial Least Squares 162 163 show that pCO<sub>2</sub> constraints on plant growth can make glacial conditions appear drier than they likely were (Wei et al., 2021). By contrast, under interglacial conditions with higher pCO<sub>2</sub> 164 levels, model experiments suggest that forest expansion in SW Iberia is mostly controlled by 165 precipitation rather than by pCO<sub>2</sub> levels (Oliveira et al., 2018; 2020). 166 Despite these advances, there is a need for additional region-based palaeoecological 167 168 research. This need was highlighted in a recent model data comparison using the BIOME4 169 model and a biome-scale reconstruction compiled from pollen records across the Northern Hemisphere (> 30°N), which reveals a level of unexplained variability in patterns across both 170 space and time (Cao et al., 2019). Detailed pollen assemblage datasets may provide key 171 insights into factors other than temperature, precipitation and potential evapotranspiration that 172 173 drive changes in vegetation dynamics and composition, such as pCO<sub>2</sub> (Ludwig et al., 2018; 174 Cao et al., 2019). 175 Recognising the role of pCO<sub>2</sub> is crucial, a key issue not only to interpret the drivers of past

ecosystems accurately, but also for anticipating how semi-arid landscapes - particularly in the

<u>Iberian Peninsula and Mediterranean region, which are is predicted to experience significantly increased aridity - will respond to ongoing climate change. The terrestrial and marine climatic</u>

176 177

indicators from the SW Iberian margin sedimentary sequences provide an extremely valuable record of environmental change, and last deglaciation vegetation changes have been widely studied here using palaeoecological records (e.g. Peyron et al., 1998; Carrión et al., 2002; Chabaud et al., 2014; Combourieu Nebout et al., 2009; Dormoy et al., 2009; Fletcher et al., 2010a; Arranbari et al., 2014; Bartlein et al., 2011; Naughton et al., 2011; 2019; Tarroso et al., 2016) and ecological niche modeling (Casas-Gallego et al., 2025). However, these are traditionally interpreted as a result of the combined effects of temperature, precipitation and evaporation changes, rather than the role of pCO<sub>2</sub>. Furthermore, few of the existing records span the entire deglaciation, or offer resolution or chronological precision to detect short-term vegetation and climate shifts in detail., and mainly focus on the mechanisms underlying the regional atmospheric and oceanic responses to the last deglaciation. to anticipate the future responses of semi-arid landscapes to ongoing climate change.

The

Here we present a new multiproxy study of IODP Site U1385 that allows athe direct comparison between terrestrial and marine climatic indicators across the LGM and deglaciation at high (centennial-scale) temporal resolution. Hence, this record provides a, and therefore, thea detailed reconstruction of vegetation changes in SW Iberia along with sea surface temperature (SST) trends in its margin during the LGM, HS1, B-A and the YD. Our This new paleoenvironmental record enablesfacenables the ilitates an will serve to exploreation of the main factors driving forest development during the LGM and the last deglaciation, and an evaluation ofe the potential pCO<sub>2</sub> thresholds for western Mediterranean forest development.

# 2. Materials and environmental setting [Figure 1]

IODP Site U1385 is a composite record of five drillings in the SW Iberian margin (37°34.285′N; 10°7.562′W, 2587 m below sea level—mbsl) located on a spur at the continental slope of the Promontório dos Príncipes de Avis, which is elevated above the abyssal plain and free from turbidite influence (Hodell et al., 2015) (Fig. 1). This work focuses on Hole A, a continuous record of 10 corrected revised meter composite depth (crmcd) mainly composed of hemipelagic silt alternating with clay (Hodell et al., 2015). For this study, Hole A was sampled from 3.84 to 1.08 crmcd, which corresponds to the period between ~21.5 and 6.4 cal\_kyra BP. The sediment supply, including pollen grains, to Site 1385 is mainly derived via fluvial transport from the Tagus and Sado hydrographic basins, providing a reliable signature of the vegetation of the adjacent continent (Naughton et al., 2007; Morales-Molino et al., 2020).

The present-day climate of southwestern Iberia is characterised by a Mediterranean climate strongly influenced by the Atlantic Ocean, Köppen classification CSa with warm summers (average ~22 °C in the warmest montharound 22 °C as the average temperature of the warmest month) mean annual temperatures between 12.5 °C \_and 17.5 °C, and mean annual precipitation from 400 \_to \_1000 mm/yr. The rainy season peaks in the winter between November and January and drought occurs in the summer generally from June to September (AEMET, 2011).

The present-day vegetation of southwestern Iberia reflects a transitional biogeographical zone between temperate and Mediterranean climates (Rivaz-Martinez et al., 2017). Coastal areas, influenced by oceanic humidity and milder winters, support thermophilous evergreen species such as *Quercus suber*, *Olea europaea* var. *sylvestris*, *Myrtus communis*, and *Pistacia lentiscus* (Asensi and Díez-Garretas et al., 2017). Inland, as elevation increases and oceanic

influence diminishes, Mesomediterranean forests dominate, composed of both evergreen (*Q. suber*, *Q. rotundifolia*, *Q. coccifera*) and deciduous oaks (*Q. faginea*, *Q. robur*), often combined with heathlands or aromatic scrublands (e.g. *Cistus* spp.). Distinctive oak–juniper woodlands appear in drier zones, and pine forests (*Pinus pinaster*, *P. pinea*) are common on sandy coastal soils. Riparian zones feature *Alnus glutinosa* and *Salix* spp., while widespread *Cistus* and *Erica* shrublands reflect the area's susceptibility to fire.

2332343. Methods

235236

237238239

240

241

242

243

244 245

246

247

248 249

250

251

252

253

254255

256257

227

228

229

230

231

232

# 3.1. Chronological framework

# [Table 1, Figure 2, Figure 3, SM Figure S1]

Sixteen AMS <sup>14</sup>C dates were used to generate a new age-model for the last deglaciation at Site U1385 (Table 1 and Fig. 2). Five of these were previously published by Oliveira et al., (2018), based on monospecific Globigerina bulloides samples and analysed at the Vienna Environmental Research Accelerator (VERA), University of Vienna, Austria. A new set of eleven samples for AMS <sup>14</sup>C analysis was selected primarily from monospecific assemblages of G. bulloides. When sample size requirements could not be met, a mixed assemblage of G. bulloides and G. inflata was used. All samples were processed at the Keck Carbon Cycle AMS Facility, University of California, Irvine (Table 1). A new set of eleven samples for AMS 14C was selected primarly from monospecific foraminifer samples of G. bulloides, when not enoughand a mixed assemblage of G. bulloides and G. inflata was processed at the Keck Carbon Cycle AMS Facility, University of California, Irvine (Table 1). The new age model, using solely the available radiocarbon dates for sedimentary record U1385 without any tuning, was calculated using a Bayesian approach through the software Bacon implemented in R (Blaauw and Christen, 2011; R Development Core Team, 2020) using the Marine 20 calibration curve (Heaton et al., 2020). The studied interval encompasses the period from ~22 to 6 ka, as shown by the radiocarbon age model (Fig. 2). The average temporal resolution for the pollen and organic biomarkers across the deglaciation is 110 and 104 years, respectively, or slightly lower (174 and 135 years, respectively) when including the Holocene section (Fig. 3 and SM Fig. S1).

258 259

#### 3.2. Pollen analysis

260261262

263264

265

266

267268

269

270

271

272273

A total of 97 samples (including 25 previously published by Oliveira et al., 2018) were analysed from 3.84 to 1.08 crmcd in Hole A, and prepared at the University of Bordeaux, France, using the standard protocol of the UMR EPOC laboratory (Georget et al., 2025). The sediment was firstly separated using coarse sieving at 150 μm, retaining the fine fraction. A sequence of chemical treatments, starting with cold HCl (hydrochloric acid) at increasing concentrations (10%, 25%, 50%), eliminated calcium carbonate particles. Followed by cold HF (hydrofluoric acid) at increasing strength (45% and 70%) to eliminate the silicates. The remaining residue was micro-sieved (10 μm mesh), retaining the coarse fraction. Exotic *Lycopodium* spore tablets of known concentration were added to each sample to calculate pollen concentrations (Stockmarr, 1971). The obtained residue was mounted in a mobile medium composed of phenol and glycerol 1% (w/v), to allow pollen/spore rotation and accurate identification. Samples were counted using a transmitted light microscope at 400X and 1000X (oil immersion) magnifications. To perform pollen identification, we used identification keys

(Faegri and Iversen, 1989; Moore et al., 1991), photographic atlases (Reille, 1992; 1995) and the SW Mediterranean modern reference collection.

The total count ranged from 198 to 1545 pollen and spores per sample, with a minimum of 100 terrestrial pollen grains and 20 pollen morphotypes to provide statistical reliability of the pollen spectra (McAndrews and King, 1976; Heusser and Balsam, 1977). The main pollen sum was calculated following previous palynological studies of Site U1385 (e.g. Oliveira et al., 2016) that excluded Pinus, Cedrus, aquatic plants, Pteridophyte and other spores, and indeterminable pollen. Aquatic plants were excluded because their abundant and local pollen comes from water bodies and can be transported far from where it grew, while Pinus and spores were excluded because their lightweight pollen wind transported may overrepresent regional vegetation. In pollen analysis, we generally excluded aquatic plants because they produce large amounts of pollen that can be carried far from water bodies, and thus do not reliably reflect local vegetation. Pinus and spores were excluded because their lightweight pollen can travel long distances, overrepresenting regional rather than local plants. The pollen percentages are calculated against the main pollen sum; but the percentages of overrepresented taxa were calculated on the basis of the main sum plus the counts for that particular individual taxon; for example: 100 \* Pinus / (Main sum + Pinus) and 100\* Cedrus / (main sum + Cedrus). Aquatic plants and spores were excluded because their abundant pollen originates in or near water bodies and can be transported far from their source, potentially overrepresenting regional vegetation. Pinus pollen, which is typically overrepresented in marine deposits, is transported by rivers from the Tagus and Sado's watersheds (Naughton et al., 2007). In contrast, the overrepresented Cedrus is transported by wind from the Atlas or Rif mountains in Morocco, were also excluded from the main sum. Aquatic plants and spores were excluded because their abundant pollen originates close or in water bodies and can be transported far from where they grew, and may overrepresent regional vegetation. Pinus pollen is generally overrepresented in marine deposits and therefore excluded from the main sum (Naughton et al., 2007). Cedrus, being an exotic component transported by wind from the Atlas or Rif mountain chains (Morocco), is also excluded. PSIMPOLL 4.27 (Bennett, 2009) was used to plot percentages for selected taxa, grouped by ecological affinities (Gomes et al., 2020). Stratigraphically constrained cluster analysis by Sum of Squares determined the five statistically significant pollen assemblage zones (U1385-1 to 5 in Fig. 3, SM Fig.1 and Table S1) based on a dissimilarity matrix of Euclidean distances with pollen taxa ≥ 1% (Grimm, 1987; Bennet et al., 2009).

In addition to the pollen-based ecological groups, we calculated the sum of Poaceae and Cyperaceae (Fig. 3g), to check the potential importance of C4 plants in the Iberian Peninsula. While most of the present-day Poaceae and Cyperaceae in this region chiefly belongs to the C3 photosynthetic-pathway plant typeplants type (Casas-Gallego et al., 2025), it is possible that C4 pathway plants were more important at other moments in recent Earth history. Pollen analysis is a core method in palaeoclimatology and palaeoecology, used to assess past climate conditions based on the ecological affinities of specific taxa grouped into pollen-based ecological groups. These groups reflect present-day vegetation—climate relationships, allowing inferences about dry, cold, warm, or moist conditions. As such, our pollen data reflect ecological responses rather than absolute quantitative climate parameters (Williams et al., 2001). A pollen diagram with clustering analysed (SM Fig. S1) was produced revealing four main episodes over the LGM and the Last deglaciation (Fig. 3, further details in SM Table S1).

### 3.3. Compilation of Iberian margin pollen records

274

275

276

277

278279

280 281

282

283

284

285

286 287

288

289 290

291

292

293

294

295

296 297

298

299

300

301 302

303 304

305 306

307

308

309

310 311

312

313

314315

316

317

In order to assess vegetation and climate changes more widely in the Iberian Peninsula region across the LGM and last deglaciation, we compiled available marine records along the Iberian margin covering the period from 23 to 6 cal.kyr BPka. Pollen count datasets from eight marine pollen records (D13882 - Gomes et al., 2020; MD03-2697 - Naughton et al., 2016; MD95-2039 - Roucoux et al., 2005; MD95-2043 Fletcher and Sánchez Goñi, 2008; MD95-2042 - Chabaud et al., 2014; ODP Site 976 - Combourieu Comborieut Nebout et al., 1998; 2002; 2009; SU81-18 Turon et al., 2003; Site U1385 - this study) were used with the original published chronologies, without any additional alignment or synchronization. Pollen percentages were recalculated against the main pollen sum. A uniform calculation of the pollen-based ecological group TMF (Temperate and Mediterranean forest) was made for each record, integrating the following taxa of 1) Temperate trees and shrubs: deciduous Quercus, Acer, Betula, Cannabis/Humulus, Carpinus, Castanea, Fraxinus excelsior-type, Hedera helix, Hippophae, Ilex, Juglans, Myrica and Vitis; and 2) Mediterranean taxa: evergreen Quercus, Quercus suber, Arbutus type, Buxus, Daphne, Jasminum, Ligustrum, Myrtus, Olea, Phillyrea, Pistacia, Rhamnus, Rhus.

To assess the general trend of vegetation patterns throughout the deglaciation, we applied a Generalised Additive Model (GAM), considered as a more robust statistical approach than loess curves (Wood, 2017; Simpson, 2018). The GAM model was fitted using the *gam*() function of the *mgcv* package (version 1.8.24; Wood, 2017) for R (version 3.6.3; R Core Team, 2020). We <u>usedfitted the model using</u> a standard GAM with REML smoothness selection, specifying with 30 basis functions (*k*=30) and a smoothing parameter of 0.0001 (*sp*=0.0001). The relatively high K allowed the model to capture potential nonlinear patterns in the data without overfitting, while the small *sp* ensured sufficient smoothness; these values were chosen after exploratory analysis and diagnostic checks. To assesscheck the validity of the smooth terms and confirm that their the used basis functions adequately captured the data wiggliness, we applied a test using the *gam.check*() function of the *mgcv* package. The resulting *k-index* was greater basis functions were used. The curve shows the fitted GAMs curves for TMF are presented, along with an approximate 95% confidence intervals (Simpson, 2018).

#### 3.4. Molecular biomarkers

 Marine biomarker analyses were carried out in 123 levels, including 30 already published by Oliveira et al., (2018). All analyses were performed following the extraction and analytical methods (Villanueva et al.,1997; Rodrigues et al., 2017). Marine coccolithophorid algae synthesise organic compounds including alkenones (Volkman et al., 1980) (Fig. 3i and j). Seawater temperature changes influence the amounts of di-, tri- and tetra-unsaturated alkenones produced by algae (Brassell et al., 1986). The use of organic solvents to separate the total lipid fraction from sediments allows the sea surface temperature alkenone-based reconstruction (U<sup>kr</sup><sub>37</sub> - SST) (e.g. Villanueva and Grimalt, 1997; Rodrigues et al., 2017). The U<sup>kr</sup><sub>37</sub> index (Prahl and Wakeman, 1987) was converted to temperatures values using the global calibration equation defined by Müller et al., (1998) with an analytical uncertainty of 0.5°C (Grimalt et al., 2001). Nevertheless, uncertainties remain, since U<sup>kr</sup><sub>37</sub> SST reconstructions may be affected by calibration biases, seasonal and ecological effects related to coccolithophorid production, and potential lateral transport or diagenetic alteration of alkenones (e.g. Conte et al., 2006; Ausín et al., 2022). As such, the derived SSTs should be regarded as robust indicators of large-scale SST trends. Additionally, tetra-unsaturated

alkenone (C<sub>37:4</sub>) percentages were calculated due to their potential to identify the occurrence of cold freshwater pulses associated with iceberg discharges (Bard et al., 2000; Martrat et al., 2007; Rodrigues et al., 2011; 2017) and therefore, changes in the reorganisation of surface water masses in the North Atlantic (Rodrigues et al., 2017).

The ratio between C<sub>29</sub> and C<sub>31</sub> n-alkanes was also calculated to understand how epicuticular wax production in terrestrial plants varied through—the time (Eglinton and Hamiltom, 1967). This index is generally considered to encompass the dynamic between woody plants and vs grasses plants of the adjacent continent (Cranwell 1973, Tareq et al., 2005, Bush et al., 2013; Struck et al., 2020). This relation encompasses the adaptation of plants, by increasing the production of-leaf wax long—chain leaf wax production, which to reduce water loss during the photosynthetic processes and prevents prevent desiccation promoted by harsh winds or more arid conditions (Bush and McInerney, 2013). Index values >1 are typically considered to reflect higher quantities of C<sub>29</sub> *n*-alkanes produced by trees and shrubs, while values <1 are generally considered to indicate higher quantities of C<sub>31</sub> *n*-alkanes by grasses and herbaceous plants (Cranwell, 1973; Rodrigues et al., 2009; Ortiz et al., 2010; ). However, the interpretation of this index may vary across biomes and depend—dependent—on source vegetation types—, and depositional processes (Carr et al., 2014; Diefendorf and Freimuth, 2017).

### 4. Results and discussion

[Figure 4, Figure 5, Table S1, SM Figure S2]

# 4.1. The effect of pCO<sub>2</sub> on biome changes during the LGM and deglaciation

Whilst a classic interpretation of ecosystem dynamics, as described for Site U1385, can be proposed solely considering the variations inof the main climatic parameters (temperature, precipitation), we hypothesise that changes in pCO<sub>2</sub> played an essential role in vegetation change, specifically in the deglacial forest expansion. Here, we evaluate the drivers of vegetation change by explicitly considering the evolution of pCO<sub>2</sub> through the deglaciation. Our discussion is supported by the present-day environmental and climatic space, considering the temperature and precipitation in which different taxa exist in the Iberian Peninsula and characterising the TMF – Quercus sp., the Heathland (ERI) - Ericaceae family and the semi-desert (STE) landscapes (SM Fig. S2).

#### 4.1.1. Last Glacial Maximum (LGM, 23-19 cal. kyr BP)

The pollen-based vegetation record from Site U1385 shows that during the LGM (pollen zone U1385-1: 21500-17990 cal. yr BP, SM Fig. S1) a grassland–heathland mosaic dominated the landscape, with semi-desert taxa (STE, ~40%) and heathland taxa (ERI, ~10–20%) (Fig. 3d, e; Fig. 4d), forming a distinctive non-analogue glacial vegetation cover.

-The prevalence of heath (*Erica* spp.) in Iberian pollen records underpins the classic view of the LGM in Iberia as a fairly humid interval, certainly compared with the extreme aridity of Heinrich stadials (Roucoux et al., 2005; Naughton et al., 2007; Fletcher and Sánchez-Goñi, 2008; Combourieu-Nebout et al., 2009; Sánchez-Goñi et al., 2009).

Nevertheless, the signals for moisture availability are somewhat complex there is a somewhat complex picture with respect to the prevailing moisture availability for vegetation during this interval. Semi-desert taxa, typically found in arid conditions, are abundant, while heathland taxa, associated with more humid environments, reach their maximum in the record (Fig. 3; SM Fig. S2c). Forest taxa weare represented in low percentages (5-15%) (Fig. 3c), suggesting

cold and relatively dry conditions over the continent. The TMF values are consistent throughout the troughout across the U1385 record and GAM-fitting to the data compilation (Fig. 3c). Similiar patterns are observed, being consistently observed across the marine records in southerly locations off the Iberian Peninsula (MD95-2043 - Fletcher and Sánchez Goñi, 2008 and ODP Site 976 - Combourieu Comborieut Nebout et al., 1998; 2002; 2009 in the Mediterranean Sea, and SU81-18- Turon et al., 2003 in the Atlantic Ocean), as well as further North off the Iberian Peninsula (MD99-2331 and MD03-2697- Naughton et al., 2007; 2016). Interestingly, the modern environmental space for the Ericaceae group (namely Erica arborea, E. australis, Calluna vulgaris) coincides with that occupied by the Quercus genus, the main constituent of the TMF group (SM Fig. S2b). This begs the question, if the environmental conditions that support heathland overlap with those for Quercus sp., then why were forests not thriving during the LGM? A possible explanation could be associated with cold atmospheric temperatures (<u>SST's average</u> SST's average ~14.5°C, Fig. 3j), even if during the LGM the temperatures were not as extreme as the ones observed during the HS1 (Bond et al., 1993; Rasmussen et al., 1996). Hence, in addition to temperature, the lowestest levels of pCO<sub>2</sub> during the LGM (ranging between 180-190 ppmv), could have been another important controlling factor, as they rank among which are among the lowest concentrations recorded during the history of land plants (Pearson and Palmer, 2000; Tripati et al., 2009). The global distribution of different vegetation types as a function of temperature and precipitation was modelled under modern conditions and for LGM pCO<sub>2</sub> (185 ppm), showing qualitative differences in the distribution of vegetation types (Shao et al., 2018). Under low pCO<sub>2</sub> grasslands were favoured to the detriment of evergreen broadleaf, evergreen and deciduous needle leaf forest. This study, however, did not include heathlands specifically, and it is not known whether this group has adaptations permitting better functioning under low pCO<sub>2</sub> levels. We speculate that drought-adapted traits in Mediterranean Ericaceae especially E. arborea including thick cuticles, small leaf size, large photosynthetic thermal window and deep root system with large diameter and a massive underground lignotuber (Gratani and Varone, 2004) may have been beneficial in coping with the challenging trade-off between photosynthesis and water loss under very low pCO<sub>2</sub>. As such, the Ericaceae of the LGM may represent part of vegetation that coped well with physiological constraints of the low pCO<sub>2</sub>. At the same time, the LGM coincides with a precession maximum, a configuration recognised

418

419 420

421

422

423

424 425

426

427

428 429

430

431

432

433

434

435

436 437

438

439 440

441

442

443

444

445 446

447

448

449 450

451

452

453 454

455

456 457

458 459

460

461

462 463

464

to reduce seasonal contrasts (i.e., reduced summer dryness) and thus favour heathland development in the Iberian Peninsula, as documented in both glacial and interglacial contexts. including the Middle to Late Holocene (Fletcher and Sánchez Goñi, 2008; Sánchez Goñi et al., 2008; Margari et al., 2014; Oliveira et al., 2017, 2018; Chabaud et al., 2014; Gomes et al., 2020). At the same time, the we note that the LGM corresponds to a maximum in the precession cycle, which is recognised to promote a weakening of seasonal contrasts (reduced summer dryness) favourable for heathland development in the Iberian Peninsula (Fletcher and Sánchez-Goñi, 2008; Sánchez-Goñi et al., 2008; Margari et al., 2014), in both glacials and interglacials (e.g. Oliveira et al., 2017), including the Middle to Late Holocene (Chabaud et al., 2014; Oliveira et al., 2018; Gomes et al., 2020). Furthermore, heathland ecosystems thrive on acidic, low-nutrient soils, which can develop as a result of altered hydrological cycles during precession maxima. The ecological advantages of Erica also include less demanding edaphic requirements (low nutrient demand), more competitive re-sprouting strategy after disturbance, including fires, as well as a higher dispersal capacity compared with Quercus sp. for example (Pausas, 2008). However, these observations do not rule out a key impact of low pCO<sub>22</sub> on vegetation composition during the LGM.

Diverse vegetation models have been used to understand the influence of climatic parameters and pCO<sub>2</sub> during the LGM (e.g. Harrison and Prentice, 2003; Woillez et al., 2011; Izumi and Bartlein, 2016; Shao et al., 2018). However, there is a disagreement about the magnitude of the pCO<sub>2</sub> influence, from being considered to have an equal influence (Izumi and Lezine, 2016) to being thought to be less critical than climatic parameters (Woillez et al., 2011; Shao et al., 2018; Chen et al., 2019). Harrison and Prentice (2003) also highlight model differences and the variable regional expression of the influence of pCO<sub>2</sub> (with higher impact in tropical areas). However, these studies agree that low pCO<sub>2</sub> had a negative physiological impact on forest development during the LGM in different continents (Jolly and Haxeltine, 1997; Cowling, 1999; Harrison and Prentice, 2003; Woillez et al., 2011; Shao et al., 2018; Chen et al., 2019). Jolly and Haxeltine (1997) used BIOME3OD to simulate LGM vs pre-industrial CO2 levels under different climatic conditions scenarios (temperature and precipitation) in tropical Africa; CO2 was considered the primary driver of biome change from tropical montane forests to shrubby heathland ecosystems. This model included a photosynthetic scheme able to simulate plant response to different levels of CO<sub>2</sub> and its impact on stomatal conductance and water stress. This study showed that increasing pCO<sub>2</sub> (above ~190 ppmv), offsets the lower temperatures (changes of -4 to -6 °C), allowing the forest to thrive and replace heathland. However, plants with higher climatic demands (temperature and precipitation), which is the case of most temperate trees, are less competitive under low pCO<sub>2</sub> conditions, compared with evergreen microphyllous species (e.g. Erica spp.).

465

466

467

468 469

470

471 472

473

474

475

476 477

478

479

480 481

482

483

484

485

486 487

488

489

490

491

492 493

494 495

496 497

498

499

500 501

502

503

504 505

506

507

508

509

510 511

512

Long-term studies considering CO<sub>2</sub> limitations on vegetation contrast in their perspectives; Gosling et al., (2022) argue that during the last 500 kyr, precipitation and fire exert the main controls on woody cover in tropical Africa while CO<sub>2</sub> effects were relatively small. In Asia, Clément et al., (2024) also emphasize the role of precipitation as the driver of vegetation distribution during interglacials, and that vegetation is not sensitive to CO<sub>2</sub> above 250 ppmv (value characterizing most of the interglacials); however, during glacial CO<sub>2</sub> conditions (<~185 ppmv), CO<sub>2</sub> is an important factor, favouring the increase of C<sub>4</sub> plants. The inclusion of pCO<sub>2</sub> in climatic reconstructions for LGM for Africa and Europe yields a wetter LGM compared with reconstructions assuming pCO<sub>2</sub> present-day concentrations (Wu et al., 2007). A similar impact is evident in the Last Glacial moisture reconstruction based on the pollen record of El Cañizar de Villarquemado in eastern Iberia; including a correction for the direct physiological effects of low pCO<sub>2</sub>, yields a wetter reconstruction of glacial climate (Wei et al., 2021). The implications of these experiments are important for the SW Iberian region and may help to solve the solveresolve the apparent contradiction between vegetation (abundance of semidesertic plants and presence of heathland) and climate simulations, which indicate enhanced winter precipitation over southern Iberian and Northwest Africa due to southward shifting of the wintertime westerlies (Beghin et al., 2016). In the absence of pCO<sub>2</sub> correction, temperature could also be misinterpreted; the LGM vegetation for Mediterranean sites was simulated and associated with warmer summers under LGM pCO<sub>2</sub>, instead of the colder conditions simulated with present-day levels of CO<sub>2</sub> (Guiot et al., 2000). In Europe, pollen reconstruction with steppe vegetation indicated warmer winter temperatures for LGM pCO<sub>2</sub> compared with the modern pCO<sub>2</sub>. (Wu et al., 2007). The bias could extend to simulations of glacial vegetation; without the pCO<sub>2</sub> effect, the cover of boreal and temperate forests is reduced, and evergreen forests are overestimated for the LGM (Woillez et al., 2011).

Experiments determining plant thresholds in response to low pCO<sub>2</sub> have not received as much attention as research on the impact of high pCO<sub>2</sub> levels (Gerhart and Ward, 2010; Dusenge et al., 2019), and to our knowledge no experimental work currently tests forest development under such low values. However, modelling approaches indicate that in C<sub>3</sub> plants,

photosynthetic capacity declines sharply once atmospheric CO<sub>2</sub> falls below ~300 ppmv, making carbon assimilation increasingly limiting for plant growth (Wagner et al., 1997). When we assess the relationship between pCO<sub>2</sub>, SST and TMF across the LGM and deglaciation events we observe that the LGM (i) corresponds to SSTs below 15.5°C and pCO<sub>2</sub> below 225 ppmv, and (ii) that TMF values remain below 20% (Fig. 5). In African mountain environments, a pCO<sub>2</sub> threshold of approximately 220 ppmv has been suggested as the minimum above which forests could develop (Dupont et al., 2019). These results suggest that Therefore, extremely low pCO<sub>2</sub> below a critical threshold of ~220-225 ppmv, played an important role in limiting may have been the critical determinant of low-forest development during in the LGM. However, we emphasize that such thresholds should not be considered universal, as they may depend on plant taxa, edaphic conditions and microclimate. Nevertheless, these These pCO<sub>2</sub> threshold values, despite differences in baseline conditions such as insolation, are broadly consistent with other time intervals where Mediterranean forest expansion occurred, for example during MIS 13 at ~216 ppmv (Oliveira et al., 2020) and MIS 18 at ~215 ppmv under relatively high temperatures and increased winter rainfall (Sánchez-Goñi et al., 2023). Temperatures during the LGM in SWsouthwestern\_Iberia may have been sufficiently mild for forest development with sea surface temperatures of ~15.5 °C (Fig. 3j) aligned with the broader threshold for forest development (Sánchez-Goñi et al., 2008). For this reason, one could speculate that a hypothetical increase in pCO2 above the observed critical threshold during the LGM could have permitted forest development in SWsouthwestern Iberia. Thus, while uncertainties remain, the convergence of multiple lines of evidence supports a key role for low pCO<sub>2</sub> in constraining forest development specially during glacial periods.

# 4.1.2. Heinrich Stadial 1 (HS1, 18.5-15 cal. kyr BP)

513

514

515

516

517

518

519

520 521

522

523 524

525 526

527 528

529

530

531

532 533

534 535

536 537

538

539 540

541 542

543

544

545

546

547 548

549

550

551

552

553

554 555

556

557

558

559 560 During HS1 (Pollen zone U1385-2: 17990 – 15230 cal. yr BP, SM Fig. S1), a Mediterranean steppe landscape (Fig. 3d) with minimum arboreal development (Fig. 3c) corresponded to the lowest SSTs of the record (SST~12°C, Fig. 3j).

The dominance of semi-desert taxa and minimum TMF (Fig. 3 and 5c) indicate the, and highest levels of aridity-are suggested by the maximum of semi-desert taxa and minimum TMF (Fig. 3 and 5c). Additionally, high C<sub>37:4</sub> alkenone values (~8.2%, Fig. 3i) reflect major meltwater pulses, associated with severe cooling in the North Atlantic during extreme cold conditions were recorded of HS1 in the Atlantic Ocean. Vegetation signals reinforce this picture of moisture stress. A sharp decrease in The notable decrease in heaths (ERI, Fig.3e) and aquatic taxa such as Isoetes as well as terrestrial marshes and wetlands (decrease in Isoetes undiff.) (SM Table S1 and SM Fig. S1) suggests significant drying of terrestrial marshes and wetlandsfurther supports increased moisture stress (SM Table S1 and SM Fig. S1). The dominance of STE during HS1 is consistent with records across the majority of the Iberian Peninsula records (Roucoux et al., 2005; Naughton et al., 2007; 2016; MD95-2043 - Fletcher and Sánchez Goñi, 2008; ODP Site 976 -- Combourieu Comborieut Nebout et al., 2002), and is reflected also in athe long-term minimum in reconstructed modelled forest levels (Fig. 3c). Throughout HS1, despite the gradual the potential effect of increaseing of pCO<sub>2</sub> (from ~185 to ~225 ppm\_between) from 18.1 to ~16 cal kyra BP (Fig. 3b), this rise was insufficientnot enough to counteract the limiting effects of extreme cold and aridity dry atmospheric conditions. Simulations with the Regional models - Weather and Research Forecast m Model that incorporate-simulating the potential vegetation with a pCO<sub>2</sub> correction show a reduction in arboreal vegetation and an expansionincrease of sparsely vegetated soils acrossfor the Iberian region during HS1 compared with the LGM (Ludwig et al., 2018). The simulated

precipitation values for SW Iberia (Tagus hydrographic basin catchment), <u>remainshow values</u>
below 700 mm/yr for HS1, which agrees with the pollen evidence for widespread semi-desert
taxa<del>development</del>.

Interestingly, the differences between HS1 and LGM concerning temperature, precipitation and pCO<sub>22</sub> are quite relevant. While pCO<sub>2</sub> levels rose modestly, the climatic extremes of HS1 - marked by severe cooling and aridity - likely drove the observed loss of heathland and constrained forest development across the peninsula. The climatic extremes of HS1, despite rising pCO<sub>2</sub>, were most likely responsible for the loss of heathland following the LGM. Besides, the forest development was constrained across the territory, and based on pollen data from marine and terrestrial records we do not observe any significant (<5% TMF) latitudinal difference when comparing northern (e.g. Peñalba et al., 1997; Perez-Obiol and Julia, 1984; Roucoux et al., 2005; Naughton et al., 2007) with southern (e.g. this study; Comborieu Nebout et al., 2002; Fletcher and Sánchez Goñi, 2008) pollen records. Furthermore, the relationship between pCO<sub>2</sub>, SST and TMF across the HS1 shows scattered values of TMF (below 20%) occurring at SST below 15.5°C and pCO<sub>2</sub> below 225 ppmv (Fig. 5), underscoring the combined climatic and physiological constraints on forest expansion.

#### **4.1.3.** Bølling-AllerødBA (BA, 15-12.5 cal. kyr BP)

(Fig. 4b and Fig. 5).

The BA (Pollen zone U1385-3: 15230 - 12780 cal. yr BP; SM Fig. S1) had generally more wereas characterised broadly by favourable climatic conditions (higher temperatures, higher moisture availability) for TMF development (Fig. 3c) including a minor increase in thermophilous Mediterranean elements (Fig. 3c and f) and a reduction of STE (Fig. 3d). The combination of warming (SST above 16°C, Fig. 3 j) and a dry to wet trend are likely the primary drivers of progressive forest development during the BA. Additionally, the increase of pCO<sub>2</sub> from ~230 to 245 ppmv should have promoted a —"fertilisation effect" during this time interval (Fig. 3b). The simulations produced by BIOME3 simulations for African Biomes (Tropical forest/Ericaceous scrub) with a present climate showed that above 190 ppmv, the increase of pCO<sub>2</sub> at intervals <20 ppmv, gradually offsets the negative effect of temperature changes. When pCO<sub>2</sub> exceeds 250 ppmv with a temperature change of ~-6°C the development of forests expand at expense of ericaceous scrubland (Jolly and Haxeltine, 1997). Within age uncertainties of the archives, abrupt increases in pCO<sub>2</sub> at 16.3 ka and 14.8 ka (Marcott et al., 2014) (Fig. 3b) could tentatively be associated with the slight increase of forest at the onset of the BA and the subsequent highest peaks of forest development observed during the BA, respectively (Fig. 3c). Cao et al. (2019), using pollen-based biome reconstruction, suggested that worldwide expansion of forests was a consequence of the increasing pCO<sub>2</sub> superimposed over the temperature increase between 21 ka and 14 ka. Cao et al. (2019) further emphasise the role of CO2 after the LGM driving a general northward expansion of forests and replacement of grassland by temperate forests in Europe. During the BA, considering that temperature and moisture availability in SW Iberia was favourable, increases in pCO<sub>2</sub> levels (>225 ppmv) may have amplified TMF expansion during this period

#### **4.1.4. Younger Dryas** (YD, 12.9 - 11.7 cal. kyr BP)

The YD (pollen zone U1385-4: 12780 – 11190 cal. yr BP, SM Fig. S1) is characterised by an initial weak forest contraction followed by its progressive expansion (Fig. 3c). At the regional scale, the landscape likely consisted of a forest–grassland mosaic, as suggested by the

relatively high presence of forest elements coexisting with semi-desert taxa (Fig. 3c, d and Fig. 4a). Strong SST cooling (Fig. 3j), (equivalent to LGM SSTs or even cooler), with a minimum of 13.2 °C in the record, without significant freshwater pulses, may have been associated with cooler land surface temperatures. However, this impact may have been muted by the positive effect of higher moisture availability (based on the presence of TMF, Naughton et al., 2019) and/or the increasing trend of pCO<sub>2</sub> (Fig. 3b). The fairly weak reduction in TMF observed in our record and corroborated by the compiled records (Fig. 3c) contrasts with the steppe environment often described for this interval, especially in the southeast of the Iberian Peninsula (Carrión et al., 2002; Camuera et al., 2019). A more pronounced forest contraction is observed in the high--altitude terrestrial/lacustrine cores (Quintanar de la Sierra II - Peñalba et al., 1997; and La Roya - Allen et al., 1996) in which the near-disappearance of the forest might reflect the altitudinal adjustments in vegetation belts (Aranbarri et al., 2014). However, the U1385 numerous Iberian records (e.g. Lake de Banyoles -- Perez-Obiol and Julià, 1994; MD03-2697 — Naughton et al., 2007; MD95-2039 — Roucoux et al., 2005; Charco da Candieira — van der Knaap and van Leeuwen, 1997; MD95-2042 — Chabaud et al., 2014; D13882 - Naughton et al., 2019; MD95-2043- Fletcher and Sánchez Goñi, 2008; ODP Site 976 — Combourieu-Comborieut Nebout et al., 2002) show a relatively high percentage of TMF during the YD compared to HS1 (Fig. 3c). Unfortunately, there is a lack of independent precipitation proxies for SW Iberia, and Dennison et al. (2018) highlight the limited una lack of reliability of in the speleothem proxies as indicators of precipitation of precipitation in this region for this time interval. More widely in the Iberian Peninsula, a double hydrological structure with a drier first phase and wetter second phase was proposed, the latter favouring the expansion of mountain glaciers (García-Ruiz et al., 2016; Baldini et al., 2019). We observe that the notable YD forest development occurred, counterintuitively, in association with similar SSTs to those of the LGM and only slightly higher than those of HS1. Along with Alongside woth higher summer insolation, higher pCO<sub>2</sub> (>240 ppmv, Fig. 5) may have been a key factor in supporting forest development. A climate simulation from transient experiments using LOVECLIM, for the site SHAK06-5K / MD01-2444 located nearby U1385, obtained a weaker AMOC, colder winter temperature, and lower precipitation for the YD compared with the LGM (Cutmore et al., 2021). This supports the scrutiny of additional factors, notably pCO2 influence on moisture availability for plants, to explain the substantial levels of TMF observed in the Iberian margin records (Fig. 3c). The increase in pCO<sub>2</sub> may have enhanced plant productivity and WUE (Cowling and Sykes, 1999; Ward et al., 2005) during the YD, partially compensating for the impact of atmospheric cooling and drying. Schenk et al. (2018) suggest pCO<sub>2</sub> may play an essential role in forestin the forest development if enough moisture is available. Tree cover may have been confined to suitable moist microhabitats and areas close to refugia; however, it was clearly less restricted than during earlier cold periods (Svenning et al., 2011), as indicated by the TMF abundances H may be that the tree cover was restricted to suitable, moist microhabitats and close to refuge zones, but it certainly was not as restricted as in previous cold periods (Svenning et al., 2011), as TMF abundances support (Fig. 3c). Simultations from vegetation-climate models based on pollen records for biome reconstruction (Shao et al., 2018) and in a dynamic vegetation model (ORCHIDEE) driven by outputs from an AOGCM (Woillez et al., 2011) emphasise the roleinfluence of increasing pCO<sub>2</sub> as a critical factor for global forestglobalworldwide forest development during the period including the YD (Shao et al., 2018). Underlying these

changes, the increase in summer insolation (Fig. 3a), which contributed to the increase of

summer temperatures and winter precipitation in the Mediterranean region (Meijer and Tuenter, 2007), cannot be neglected as a driverpremeteror of forest development, at least

609

610 611

612

613

614 615

616

617

618

619

620

621 622

623

624 625

626

627 628

629

630 631

632

633

634

635

636

637

638

639

640 641

642

643

644

645 646

647 648

649 650

651

652

653 654

655

where trees were not excessively water-stressed. However, disentangling the contribution of insolation vs pCO<sub>2</sub> requires sensitivity experiments, not yet performed. In summary, the persistence of TMF during the YD, despite colder winters and drier summer conditions compared to the B-A, sis most plausibly explained by eems to be best explained by the combined interaction between precipitation variability, maximum insolation and increasing pCO<sub>2</sub> (between ~245 and 265 ppmv) (Fig. 4a).

### 4.1.5 Early to Middle Holocene (11.7-4.2 cal. kyr BP)

Pollen zone U1385-5 (11190 – 4260 cal yr BP) corresponds to the Early to Middle Holocene. This <u>interval isintervalzone is</u> marked by the expansion of TMF and thermofilous Mediterranean elements, reflecting a regional increase in temperature and precipitation <u>in parallel with alongside</u> warm SSTs (>18°C). Despite <u>coarserthe low</u> temporal resolution for this interval, the U1385 record is consistent with nearby records showing a maximum forest development at <u>raround</u> 9000 cal yr B.P. (Fig. 3c). <u>The noting that the</u> specific timing of the Holocene forest maximum varied across the Iberian Peninsula along a gradient of regional moisture availability (Gomes et al., 2020). The Early Holocene pCO<sub>2</sub> exceeded 260 ppmv, representing full interglacial conditions. The combination of coupled interglacial ocean-atmosphere conditions (reflected in high SSTs) and high pCO<sub>2</sub> supported maximum forest development (Fig. 5). The impact on <u>plant moisture availability for plants compared to the preceding glacial conditions would have been profound, supporting high productivity and further increases in WUE. The progressive lifting of CO<sub>2</sub> constraints on photosynthesis throughout <u>across</u> the Last Deglaciation thus may thus represent an important factor underlying the forest development in SW Iberia.</u>

# 4.2. C<sub>29</sub>/C<sub>31</sub> ratio and C<sub>3</sub>/C<sub>4</sub> dynamics: potential and limitations

Long-chain alkanes with odd-numbersed n-alkane, such as C<sub>29</sub>, C<sub>31</sub>, C<sub>33</sub>, are epicuticular waxes produced by terrestrial plants. In lake sediments, higher abundance of, with C29 occurs in catchments with more trees, while higher abundance of while grassy catchments often representing woody plants and C<sub>31</sub> is observed in grassy catchmentses (Meyers, 2003). However, caution is required when interpreting C<sub>29</sub>/C<sub>31</sub> in taxonomic terms because both woody plants (trees and shrubs) and grasses can produce C<sub>29</sub> and C<sub>31</sub> chain lengths (Ortiz et al., 2010; Bush and McInerney, 2013). Additionally, n-alkane chain-length patterns differ across species and environments, so C<sub>29</sub>/C<sub>31</sub> ratios cannot be interpreted as strict woody vs. grass markers (Bush and McInerney, 2013). Insights into the dominance of different plant physiological pathways in response to contrasting levels of pCO2 and humidity can be potentially gained by analysing using C<sub>29</sub>/C<sub>31</sub> n-alkanes from of Site U1385. The C<sub>29</sub>/C<sub>31</sub> ratio<del>curve</del> shows important variability between climatic phases, with increasing values during the LGM, high values during HS1 and the YD, and lower values during the BA and Holocene (Fig. 3h). The  $C_{29}/C_{31}$  ratio is positively correlated (Pearson's correlation coefficient, r =-0.52, p-value =-2.473e-08) with the STEsemidesert pollen group and negatively correlated (r =--0.63, p-value =-2.821e-12) with TMF (Fig. 3c, d and h), indicating a link between pollen-based vegetation changes and n-alkane chain-length distributions. Notably, the expected simple interpretation of C<sub>29</sub>/C<sub>31</sub> as "trees vs grasses" does not appear to hold for this dataset across the different phases. These observations support a coherent link between pollen-based vegetation changes on the adjacent continent and n-alkane chain-lengths. In general, C29 and C<sub>31</sub>, as well as other long-chain alkanes with odd carbon numbers (e.g. C<sub>29</sub>, C<sub>31</sub>, C<sub>33</sub>), are

epicuticular waxes produced by terrestrial plants, from which C29 could represent woody plants and C<sub>31</sub> grasses (Meyers, 2003). However, caution in interpreting the C<sub>29</sub>/C<sub>31</sub> ratio in terms of taxonomic groups is required since woody plants and grasses are both capable of producing C<sub>29</sub> and C<sub>31</sub> chain lengths (Ortiz et al., 2010; Bush and McInerney, 2013). Furthermore, differences are observed between global regions and biomes in terms of what long-chain nalkanes a species produces (Bush and McInerney, 2013). Here, we do not find that the anticipated general interpretation of the C<sub>29</sub>/C<sub>3+</sub> ratio as an indicator of the relative abundance of trees vs grasses holds for our datasets. We propose Instead, we offer We propose two possible interpretations, which may explain the observed C29/C31 variability. First:,.1) First a physiological stress response hypothesis: the C<sub>29</sub>/C<sub>31</sub> ratio in this setting may reflect an adaptation of plants to aridity. The NnLeaf-waxes n-alkanes of leaf waxes are produced to protect plants against the loss of water during the photosynthesistic process (Post-Beittenmiller, 1996; Jetter et al., 2006). We could expect that arid, cold and windy conditions impose greater physiological stress onto be more disturbing for woody plants than on grasses; with demanding physiological requirements requirements compared to grasses. Therefore, such harsh environments could exert greater stress on woody plants than on herbaceous taxa. Consequently, the increases inef the C29/C31 values during HS1 and YD, may could suggest that a climatic adaptation of woody plants (TMF and ERI) responded to climatic stress by enhancing increasing the production of leaf wax C<sub>29</sub> production as a protective strategy to survive under these challenging conditions (Fig. 3h). Second, a vegetation compositional shift response: alternatively, changes in C<sub>29</sub>/C<sub>31</sub> may reflect the shifts thatin chain-lengths may reflect compositional shifts between woody-dominated vegetation diversewiththat includes diverse ecological tolerances, ranging from from semi-desert dwarf shrubs such as Artemisia to mesophyll broad-leaved trees. In this contextAs such, a prevailing "trees vs grasses" interpretative frameworkstructure may not be adequately represent therepresente for the Iberian vegetation patternsPeninsula setting. We stress that both hypotheses are plausible but require further validation. Nevertheless, the coherent climate signal observed in the U1385 record is encouraging for future studies aimed at linking leafwax chemistry of contributing species and vegetation dynamics in this region (Cutmore, 2021). The traditional taxonomic generalisation of C<sub>29</sub> woody versus C<sub>34</sub> grasses (Meyers, 2003), still needs some caution and further research to develop a fuller picture of the leaf-wax characteristics of contributing species in the region is required (Cutmore, 2021). However, the coherent climate signature evident in the U1385 is encouraging for this endeavour. Other hypotheses to be explored for understanding the role of different forcings on the Mediterranean forest development during deglaciations include the connection between the long-chain n-alkanes and the dynamic between C<sub>3</sub> and C<sub>4</sub> plants. Beyond taxonomic shifts, the link between n-alkane chain-length distributions and the C<sub>3</sub>/C<sub>4</sub> plant dynamic is also relevant. Nowadays, African savannahs are dominated by C<sub>4</sub> plants, and biomarkers (including C<sub>31</sub> n-alkanes) have been associated with can be used to infer their presence in past landscapes (Dupont et al., 2019). Worldwide, 80% of Poaceae (grasses) and Cyperaceae (sedges) usepresent a C<sub>4</sub> photosynthetic pathway that is favoured by arid conditions (Sage, 2017). However Unfortunately. pollen analysis cannot discriminate between Poaceaediscriminate Poaceae and Cyperaceae pollen morphotypes exclusivelymorphotypes from exclusively or in its majority of C<sub>4</sub> plants. We have grouped the Poaceae and the Cyperaceae pollen taxa, noting the inherent limitations of this grouping to represent C<sub>4</sub> C4 plants in Iberia as we know that C<sub>3</sub> are the dominant grasses across the region less than 10% of the grasses in this region belong to C4 plants at present (Casas-Gallego et al., 2025) (Fig. 3g). Accordingly, the grouping of Poaceae + Cyperaceae pollen must be interpreted with

705

706

707

708

709

710 711

712

713 714

715

716 717

718

719

720

721

722 723

724

725

726

727

728

729

730

731

732 733

734

735

736 737

738

739

740 741

742

743

744 745

746

747

748 749

750

751

caution. During Across the last deglaciation, this group (Poaceae + Cyperaceae) showspresents relatively high but fluctuating values with considerable oscillations between the LGM and the BA and more stable behaviour onwards stabilising thereafter, without a clear correlation with other proxies (TMF, STE, or C29/C31). No particular correlation with other indicators (TMF, or STE, or C<sub>29</sub>/C<sub>31</sub>) was evident, apart from the apparent instability before the Holocene. Therefore, we do not observe particular evidence to suggest an increased importance of grasses and sedges during arid intervals or low pCO2 intervals of the LGM and deglaciation. Thus, we do not find strong evidence for an increased role of grasses/sedges, or of C4 plants specifically, during arid or low pCO<sub>2</sub> intervals. Experimental studies In laboratory studies, show that C<sub>3C3</sub> grasses outperform C<sub>4C4</sub> grasses when temperatures rise by 5 to 15°C at a low CO<sub>2</sub> concentration of 200 ppm. Research on the quantum yield of photosynthesis identified a "crossover temperature"—the point at which  $C_{3C_3}$  and  $C_{4C_4}$  plants perform equally. This crossover depends on both temperature and CO<sub>2</sub> levels. Modelling across 0\_-45°C and  $CO_2$  levels from 150-700 ppm shows that whether  $C_3$ - $C_3$  or  $C_{4C4}$  plants are favoured is determined by the interaction between these two factors, unfortunately humidity humidity was not considered (Ehleringer et al., 1997; Edwards et al., 2010). Since Furthermore, most of the C<sub>4C4</sub> plants are confined to the tropical grasslands and savannahs; being better adapted to environments with higher temperatures, aridity, poor nutrient poor environments with intensive with and intensive disturbance caused by animals or fire regimes (Bond et al., 2005; Edwards et al., 2010). Likewise, one should expect that vegetation in SW Iberia after the LGM (Fig. 3 and 5) should be dominated bedominated by mainly composed of C<sub>3</sub> plants. This interpretationinterpreation is consistent with the relatively cold SSTs; considering the estimated SSTs indicating relatively cold temperatures (Fig. 5) and the high percentages of Artemisia spp (C<sub>3</sub> plant) in the pollen record (SM Fig. S1).

753 754

755

756 757

758

759 760

761

762

763 764

765

766

767

768

769 770

771

772 773

774

775

776

777

778

779

780 781

782

783

784

785

786

787

788 789

790

791

792 793

794

795

796 797

798

However, it is not currently possible to completely entirely rule out an role irolencreased importance of C<sub>4</sub> plants in the glacial vegetation of SW Iberia, because pollen morphology does not allow the separation of these groups. Stable isotope studies on ancient grass pollen were able to discriminate of discriminate The discrimination of C<sub>3</sub>/C<sub>4</sub> grasses, but single-grain analyses remain technically challenging. with challenges at the single grain measurements has been made on the basis of stable isotopes of ancient grass pollen (Nelson et al., 2016), although the single-grain isotopic measurements employed remain technically challenging to implement. There is aimportant scope for further study of biomarker proxies to clarify the dynamic between C<sub>3</sub>/C<sub>4</sub> plants in the Temperate/Mediterranean (Warm-temperate) biomes. This highlights the fact that C<sub>3</sub>/C<sub>4</sub> plant dynamics observed in Africa (e.g. Dupont et al., 2019) and other savannahs ecosystems are notis not replicable in our study area so far. Biomarker species/groups fingerprinting studies are required in order to distinguish between C<sub>3</sub> and C<sub>4</sub> plants and test for an increased abundance of C<sub>4</sub> plants within Iberian Mediterranean ecosystems during the last deglaciation. Further biomarker research is therefore needed to resolve C<sub>3</sub>/C<sub>4</sub> dynamics in temperate–Mediterranean biomes. Current evidence suggests that the C<sub>3</sub>/C<sub>4</sub> shifts documented in African savannahs (e.g., Dupont et al., 2019) are not directly applicable to our study area. Species-level biomarker fingerprinting will be essential to test whether C<sub>4</sub> plants played a significant role in Iberian Mediterranean ecosystems during the last deglaciation.

In summary, although future isotopic and biomarker approaches hold great promise for resolving C<sub>3</sub>/C<sub>4</sub> dynamics, the current evidence strongly supports C<sub>3</sub> dominance in SW Iberia during the deglaciation. This interpretation is consistent with the modern distribution of plants

in the region, where less than 10% of grasses are C4 (Casas-Gallego et al., 2025), and with the prevailing cool and humid conditions of the LGM and YD, which favor favour C<sub>3</sub> over C<sub>4</sub> photosynthesis. Thus, while acknowledging the limitations of pollen-based proxies, the available data indicate that C<sub>3</sub> plants were the dominant contributors to the Iberian vegetation signal.

#### 5. Conclusion

This study presents high-resolution pollen and biomarkersSST records from Site U1385 off the SW Iberian Margin, providing new insights into vegetation dynamics during key climate transitions of the last deglaciation and the associated pCO<sub>2</sub> changes effering valuable data for understanding past vegetation dynamics during key climate transitions and pCO<sub>2</sub> changes of the LGM and deglaciation. We applied a biomarker proxy (leaf wax C<sub>29</sub>/C<sub>31</sub> ratio), which is positively correlated with the semi-desert pollen curve and a negatively correlatedion with TMF, we demonstratinge its potential as an indicator of aridity in marine cores of the Western Mediterranean region. We applied a biomarker proxy (leaf wax C<sub>29</sub>/C<sub>31</sub> ratio), which is positively correlated with the semi-desert pollen curve and negatively with TMF, we demonstrate revealing its potential as a proxy of aridity in the Mediterranean region). The high temporal resolution of the record, combined with a analysis and robust radiocarbon chronology, enables allow consistent and more accurate comparisons with regional datasets, strengthening its making this study a valuable contribution for future palaeoenvironmental palaeonvironmental reconstructions and model simulations.

Rather than simply interpreting our dataset in terms of past temperature and precipitation changes, we examine the U1385 record In the context of the bodyan increasing in light of the growing corpus of modern and palaeo observational and modelling studies that support a significant influence of pCO<sub>2</sub> on past vegetation distribution and composition. During the LGM, cold temperatures, low seasonality, and strong physiological drought stress under low pCO<sub>2</sub> restricted forest growth and favoured heathlands. We suggest that low pCO2 acted as a modulator of vegetation response during the LGM. Cold temperatures, low seasonality, and exacerbated drought stress resulting from plant physiological impacts of low pCO2 likely restricted forest growth while favouring heathlands. Traits of Mediterranean Ericaceae, such as deep roots and thick waxy leaves, may have given these plants a competitive advantage. During HS1, woody vegetation was significantly suppressed due to cold and arid conditions, exacerbated by low atmospheric pCO2 levels. The subsequent netable expansion of temperate Mediterranean forests (TMF) during the Bølling-Allerød (BA) was promoted by warmer, wetter conditions and was driven by warmer and moister conditions, and also favoured by rising pCO<sub>2</sub> concentrations. During the Younger Dryas (YD), despite a return to colder temperatures, forest-grassland mosaics persisted primarily supported by adequateincreased moisture availability and sustained higher pCO<sub>2</sub> levels.

Furthermore, our study suggests a critical pCO<sub>2</sub> threshold for forest expansion at ~225 ppmv.study supports a critical pCO<sub>2</sub> threshold for forest expansion during the deglaciation at ~225 ppmv. Below this value (e.g. LGM and HS1), arboreal populations were generally restricted in their development withbeing the (e.g. LGM) and the impact of climatic aridification and cooling (e.g. HS1) was being detrimental. Above this value, forestsforets expanded arboreal populations developed strongly (e.g. during the BA) and and the effects of adverse climatic conditions the impact of climatic deterioration (e.g. during the YD) was buffered moderated. This threshold value is consistent with aligns with several observations

from Mediterranean to tropical to the tropical African environments (e.g. Dupont et al., 2019; Oliveira et al., 2020; Koutsodendris et al., 2023; Sánchez-Goñi et al., 2023). The concept should be further tested in regional vegetation models to determine the vegetation response to pCO2 fluctuations during past cold periods.

Finally, our Our findings highlight the importance of pCO<sub>2</sub> as a key driver of vegetation change in the Mediterranean region through its control on plant moisture-availability and water-use efficiency use efficiency its influence on moisture availability in plants (Koutsodendris et al., 2023). These palaeo-data provide critical context for understanding vegetation responses under future climate scenarios with rising CO<sub>2</sub> and shifting precipitation regimes. offer valuable context for elucidating vegetation responses under future climate scenarios involving rising CO<sub>2</sub> and shifting precipitation patterns. At the same time, they underscore the need for further research on the relationship between long-chain n-alkanes, vegetation types, and C<sub>3</sub>/C<sub>4</sub> plant dynamics, as the long-chain alkanes do not yet provide a reliable basis to disentangle the dynamics between woody plants and grasses in the Mediterranean ecosystems.

since long-chain alkanes currently offer only limited capacity to disentangle woody vs. grassy contributions in Mediterranean They also highlight the need for further investigation of the relationship between long-chain *n*-alkanes and present day vegetation and the C<sub>3</sub>/C<sub>4</sub>-plants ratio as the long-chain alkanes do not yet provide a reliable basis to disentangle the dynamics between woody plants and grasses in the Mediterranean domain.

#### **Author contribution**

 SDG, WF, FN and AS contributed to the conception and design of the study, data analysis and interpretation. Also they were responsible for the grant application to NERC. SDG performed pollen analysis. TR performed biomarkers analysis. AR <u>performed performed assemblage for a figure 1.</u> SDG prepared the original draft and wrote the manuscript including figures with the critical input (edition and revision) from all co-authors.

#### **Data** accessibility

The data supporting the findings of this study will be made available upon publication. Interested researchers can access the data by contacting the first author directly or through a publicly accessible data repository.

### **Competing interests**

The authors declare that they have no conflict of interest.

# Acknowledgements

This research was supported by the Portuguese Foundation for Science and Technology (FCT) SFRH/BD/128984/2017 PhD grant to SDG, the ULTImATum (IF/01489/2015) and, the Hydroshifts (PTDC/CTA-CLI/4297/2021) projects; CCMAR FCT Research Unit - project UIDB/04326/2020, CCMAR BCC grant (Incentivo/MAR/LA00015/2014) to FN, FCT contract (CEECIND/02208/2017) to DO, WarmWorld Project (PTDC/CTA-GEO/29897/2017) for

890 Biomarker analyses, and grant (SFRH/BPD/108600/2015) to TR. The sixteen radiocarbon dates were obtained through the NERC radiocarbon allocations 2136.1018 and 2199.1019. 891 The contributions of L. Devaux are gratefully acknowledged (Bordeaux 1 University, EPOC, 892 UMR-CNRS 5805) for his assistance in palynological treatments. This study received 893 894 Portuguese national funds from FCT - Foundation for Science and Technology through (DOI:10.54499/UIDB/04326/2020) 895 UIDB/04326/2020 and LA/P/0101/2020 (DOI:10.54499/LA/P/0101/2020). 896

# References

897 898 899

900 901

902 903

904

905 906

907

908

909

910

911 912

913

914

915

916

920

921 922

923

924

925

Agencia Estatal de Meteorología (AEMET) and Instituto de Meteorologia (IM, Portugal): Atlas Climático Ibérico: Temperatura del aire y precipitación (Experiment Normais 1971–2000), AEMET & IM, Gobierno de España, Madrid and Lisbon, ISBN 978-84-7837-079-5, 2011.

- Allen, J.R., Huntley, B., and Watts, W.A.: The vegetation and climate of northwest Iberia over the last 14,000 years, J Quaternary Sci., 11,125-147, https://doi.org/10.1002/(SICI)1099-1417(199603/04)11: 2<125:AID-JQS232>3.0. C.O.;2-U, 1996.
- Alley, R.B. and Clark, P.U.: The deglaciation of the northern hemisphere: a global perspective, Annu Rev Earth Pl Sc, 27, 149-182, https://doi.org/10.1146/annurev.earth.27.1.149, 1999.
- Aranbarri, J., González-Sampériz, P., Valero-Garcés, B., Moreno, A., Gil-Romera, G., Sevilla-Callejo, M., García-Prieto, E., Di Rita, F., Mata, M.P., Morellón, M., and Magri, D.: Rapid climatic changes and resilient vegetation during the Lateglacial and Holocene in a continental region of south-western Europe, Global Planet. Change, 114, 50-65, https://doi.org/10.1016/j.gloplacha.2014.01.003, 2014.
- Asensi, A. and Díez-Garretas, B.: Coastal Vegetation, in The Vegetation of the Iberian Peninsula, edited by: Loidi, J., Plant and Vegetation, vol. 13, Springer, Cham, Switzerland, pp. 397–432, https://doi.org/10.1007/978-3-319-54867-8\_8, 2017.
- 917 Ausín, B., Haghipour, N., Bruni, E., and Eglinton, T.: The influence of lateral transport on 918 sedimentary alkenone paleoproxy signals, Biogeosciences, 19, 613–627, 919 https://doi.org/10.5194/bg-19-613-2022, 2022.
  - Bard, E., Arnold, M., Maurice, P., Duprat, J., Moyes, J., and Duplessy, J.C.: Retreat velocity of the North Atlantic polar front during the last deglaciation determined by <sup>14</sup>C accelerator mass spectrometry, Nature, 328, 791, https://doi.org/10.1038/328791a0, 1987.
  - Bard, E., Rostek, F., Turon, J.L., and Gendreau, S.: Hydrological impact of Heinrich events in the subtropical northeast Atlantic, Science, 289, 1321-1324, 10.1126/science.289.5483.1321, 2000.
- Bartlein, P.J., Harrison, S.P., Brewer, S., Connor, S., Davis, BAS., Gajewski, K., Guiot, J., Harrison-Prentice, T.I., Henderson, A., Peyron, O., and Prentice, I.C.: Pollen-based continental climate reconstructions at 6 and 21 ka: a global synthesis, Clim. Dynam., 37, 775-802, https://doi.org/10.1007/s00382-010-0904-1, 2011.
- Beghin, P., Charbit, S., Kageyama, M., Combourieu-Nebout, N., Hatté, C., Dumas, C., and
   Peterschmitt, J.-Y.: What drives LGM precipitation over the western Mediterranean? A
   study focused on the Iberian Peninsula and northern Morocco, Clim. <a href="Dynam.46">Dynam. 46</a>
   2611-2631, https://doi.org/10.1007/s00382-015-2720-0, 2016.
- Bennett, K.D.: Documentation for Pesimpoll 4.27 and Pescomb 1.03: C programs for plotting and analysing pollen data, http://www.chrono.qub.ac.uk/psimpoll/psimpoll.html,2009.

- Blaauw, M. and Christen, J.A.: Flexible paleoclimate age-depth models using an autoregressive gamma process, Bayesian Anal., 6, 457-474, 10.1214/ba/1339616472, 2011.
- Boessenkool, K. P., Brinkhuis, H., Schönfeld, J., and Targarona, J.: North Atlantic sea-surface temperature changes and the climate of western Iberia during the last deglaciation; a marine palynological approach, Global Planet. Change, 30, 33-39, 10.1016/S0921-8181(01)00075-3, 2001.
- Bond, W.J., Woodward, F.I. and Midgley, G.F.: The global distribution of ecosystems in a world without fire, New phytologist, 165, 525-538, https://doi.org/10.1111/j.1469-8137.2004.01252.x, 2005
- 946 Brassell, S.C., Eglinton, G., Marlowe, I.T., Pflaumann, U., and Sarnthein, M.: Molecular 947 stratigraphy: a new tool for climatic assessment, Nature, 320, 129-133, 948 https://doi.org/10.1038/320129a0, 1986.
- Bush, R.T. and McInerney, F.A.: Leaf wax n-alkane distributions in and across modern plants: implications for paleoecology and chemotaxonomy, Geochim. Cosmochim. Ac., 117, 161-179, 2013.
- Camuera, J., Jiménez-Moreno, G., Ramos-Román, M.J., García-Alix, A., Toney, J.L., Anderson, R.S., Jiménez-Espejo, F., Bright, J., Webster, C., Yanes, Y., and Carrión, J.S.: Vegetation and climate changes during the last two glacial-interglacial cycles in the western Mediterranean: A new long pollen record from Padul (southern Iberian Peninsula), Quaternary Sci. Rev., 205, 86-105, https://doi.org/10.1016/j.quascirev.2018.12.013, 2019.
- Cao, X., Tian, F., Dallmeyer, A., and Herzschuh, U.: Northern Hemisphere biome changes (> 30° N) since 40 cal ka BP and their driving factors inferred from model-data comparisons, Quaternary Sci. Rev., 220, 291-309, https://doi.org/10.1016/j.quascirev.2019.07.034, 2019.
- Carlson, A. E., LeGrande, A. N., Oppo, D. W., Came, R. E., Schmidt, G. A., Anslow, F. S., Licciardi, J. M., and Obbink, E. A.: Rapid early Holocene deglaciation of the Laurentide ice sheet, Nature Geosci., 1, 620–624, https://doi.org/10.1038/ngeo285, 2008.
- Carr, A. S., Boom, A., Grimes, H. L., Chase, B. M., Meadows, M. E., and Harris, A.: Leaf wax n-alkane distributions in arid zone South African flora: environmental controls, chemotaxonomy and palaeoecological implications. Org. Geochem., 67, 72–84, https://doi.org/10.1016/j.orggeochem.2013.12.004, 2014.
- Carrión, J.S.: Patterns and processes of Late Quaternary environmental change in a montane region of southwestern Europe, Quaternary Sci. Rev., 21, 2047-2066. 10.1016/S0277-3791(02)00010-0, 2002.
- Casas-Gallego, M., Postigo-Mijarra, J. M., Sánchez-de Dios, R., Barrón, E., Bruch, A. A., Hahn, K., and Sainz-Ollero, H. (2025). Changes in distribution of the Iberian vegetation since the Last Glacial Maximum: A model-based approach. Quaternary Sci. Rev., 351, 109162, https://doi.org/10.1016/j.quascirev.2024.109162, 2025.
- 975 Chabaud, L., Sánchez Goñi, M.F., Desprat, S., and Rossignol, L.: Land-sea climatic variability 976 in the eastern North Atlantic subtropical region over the last 14,200 years: Atmospheric and 977 different timescales, The Holocene, oceanic processes at 24, 787-797, https://doi.org/10.1177/0959683614530439, 2014. 978
- Chen, W., Zhu, D., Ciais, P., Huang, C., Viovy, N., and Kageyama, M.: Response of vegetation cover to CO2 and climate changes between Last Glacial Maximum and pre-industrial period in a dynamic global vegetation model, Quaternary Sci. Rev., 218, 293-305, https://doi.org/10.1016/j.quascirev.2019.06.003, 2019.

- Chevalier, M., Davis, B. A. S., Heiri, O., Seppä, H., Chase, B. M., Gajewski, K., Lacourse, T.,
- Telford, R. J., Finsinger, W., Guiot, J., Kühl, N., Maezumi, S. Y., Tipton, J. R., Carter, V. A.,
- Brussel, T., Phelps, L. N., Dawson, A., Zanon, M., Vallé, F., Nolan, C., Mauri, A., de Vernal,
- A., Izumi, K., Holm ström, L., Marsicek, J., Goring, S., Sommer, P. S., Chaput, M., and
- 887 Kupriyanov, D.: Pollen-based climate reconstruction tech niques for late Quaternary
- 988 studies, Earth Sci. Rev., 210, 103384, https://doi.org/10.1016/j.earscirev.2020.103384,
- 989 2020.
- Chevalier, M., Chase, B. M., Quick, L. J., Dupont, L. M., and Johnson, T. C.: Temperature change in subtropical southeastern Africa during the past 790,000 yr, Geology, 49, 71–75,
- 992 https://doi.org/10.1130/G47841.1, 2021.
- 993 Clark, P.U., Shakun, J.D., Baker, P.A., Bartlein, P.J., Brewer, S., Brook, E., Carlson, A.E.,
- Cheng, H., Kaufman, D.S., Liu, Z., and Marchitto, T.M.: Global climate evolution during the
- 995 last deglaciation. P. Natl. Acad. Sci. USA, 109, E1134-E1142,
- 996 https://doi.org/10.1073/pnas.1116619109, 2012
- 997 Claussen, M., Selent, K., Brovkin, V., Raddatz, T., and Gayler, V.: Impact of CO2 and climate
- on Last Glacial Maximum vegetation A factor separation, Biogeosciences, 10, 3593-3604,
- 999 10.5194/bg-10-3593-2013, 2013.
- 1000 Cleator, S.F., Harrison, S.P., Nichols, N.K., Prentice, I.C., and Roulstone, I.: A new
- multivariable benchmark for Last Glacial Maximum climate simulations. Clim. Past, 16, 699-
- 712, https://doi.org/10.5194/cp-16-699-2020, 2020.
- 1003 Clément, C., Martinez, P., Yin, Q., Clemens, S. C., Thirumalai, K., Prasad, S., Anupama, K.,
- Su, Q., Lyu, A., Grémare, A., & Desprat, S.: Greening of India and revival of the South
- Asian summer monsoon in a warmer world. Commun. Earth Environ., 5(1), 685, 2024.
- 1006 Combourieu Nebout, N., Peyron, O., Dormoy, I., Desprat, S., Beaudouin, C., Kotthoff, U., and
- Marret, F.: Rapid climatic variability in the west Mediterranean during the last 25 000 years
- from high resolution pollen data, Clim. Past, 5, 503-521, https://doi.org/10.5194/cp-5-503-
- 1009 2009, 2009.
- 1010 Conte, M. H., Sicre, M.-A., Rühlemann, C., Weber, J. C., Schulte, S., Schulz-Bull, D., and
- Blanz, T.: Global temperature calibration of the alkenone unsaturation index (UK'37) in
- surface waters and comparison with surface sediments, Geochem. Geophys. Geosyst., 7,
- 1013 Q02005, https://doi.org/10.1029/2005GC001054, 2006.
- 1014 Cowling, S.A. and Sykes, M.T.: Physiological significance of low atmospheric CO<sub>2</sub> for plant-
- 1015 climate interactions, Quaternary Res., 52, 237-242,
- 1016 https://doi.org/10.1006/qres.1999.2065, 1999.
- 1017 Cowling, S.A.: Simulated effects of low atmospheric CO2 on structure and composition of
- North American vegetation at the Last Glacial Maximum, Global Ecol. Biogeogr., 8, 81-93,
- https://doi.org/10.1046/j.1365-2699.1999.00136.x, 1999.
- 1020 Cranwell, P.A.: Chain-length distribution of n-alkanes from lake sediments in relation to post-
- 1021 glacial environmental change, Freshwater Biology, 3, 259-265,
- https://doi.org/10.1111/j.1365-2427.1973.tb00921.x, 1973.
- 1023 Cruz-Silva, E., Harrison, S. P., Prentice, I. C., Marinova, E., Bartlein, P. J., Renssen, H., and
- Zhang, Y.: Pollen-based reconstructions of Holocene climate trends in the eastern
- 1025 Mediterranean region. Clim Past, 19(11), 2093-2108, https://doi.org/10.5194/cp-19-2093-
- 1026 2023, 2023.
- 1027 Cutmore, A. V.: Insights into the nature of climate and vegetation changes over the last 28,000
- years using combined pollen and leaf-wax biomarker analyses from the SW Iberian Margin,
- Doctoral dissertation, UCL (University College London), 2021.

- Cutmore, A., Ausín, B., Maslin, M., Eglinton, T., Hodell, D., Muschitiello, F., ... & Tzedakis, P. 1030
- 1031 C.: Abrupt intrinsic and extrinsic responses of southwestern Iberian vegetation to millennial-
- 28 1032 variability over the past ka. J. Quat. Sci.. 37(3), https://doi.org/10.1002/jqs.3392, 2022.
- 1033
- Davis, B. A. S., Fasel, M., Kaplan, J. O., Russo, E., and Burke, A.: The climate and vegetation 1034
- of Europe, North Africa and the Middle East during the Last Glacial Maximum (21 000 yr BP) 1035
- based on pollen data, Clim. Past, 20, 1939-1988, https://doi.org/10.5194/cp-20-1939-1036 1037 2024, 2024.
- 1038 Denniston, R.F., Houts, A.N., Asmerom, Y., Wanamaker Jr, A.D., Haws, J.A., Polyak, V.J.,
- Thatcher, D.L., Altan-Ochir, S., Borowske, A.C., Breitenbach, S.F. and Ummenhofer, C.C., 1039
- 2018. A stalagmite test of North Atlantic SST and Iberian hydroclimate linkages over the 1040 last two glacial cycles. Climate of the Past, 14. Doi: 10.5194/cp-14-1893-2018 1041
- 1042 Denton, G. H. and Hughes, T. J.: The Last Great Ice Sheet, Wiley Interscience, New York, 1043 484 pp., ISBN 9780471065383, 1981.
- Denton, G.H., Anderson, R.F., Toggweiler, J.R., Edwards, R.L., Schaefer, J.M., and Putnam, 1044
- A.E.: The last glacial termination, Science, 328, 1652-1656, 10.1126/science.1184119, 1045 1046 2010.
- Diefendorf, A. F., & Freimuth, E. J.: Extracting the most from terrestrial plant-derived n-alkyl 1047
- lipids and their carbon isotopes from the sedimentary record: a review. Org. Geochem., 1048
- 103, 1-21, https://doi.org/10.1016/j.orggeochem.2016.10.016, 2017. 1049
- 1050 Dormoy, I., Peyron, O., Combourieu Nebout, N., Goring, S., Kotthoff, U., Magny, M., and
- Pross, J.: Terrestrial climate variability and seasonality changes in the Mediterranean 1051
- 1052 region between 15 000 and 4000 years BP deduced from marine pollen records, Clim.
- 1053 Past, 5, 615-632, https://doi.org/10.5194/cp-5-615-2009, 2009.
- 1054 Dupont, L.M., Caley, T., and Castañeda, I.S.: Effects of atmospheric CO2 variability of the
- 1055 past 800 kyr on the biomes of southeast Africa, Clim. Past, 15, 1083-1097, 1056 https://doi.org/10.5194/cp-15-1083-2019, 2019.
- 1057 Dusenge, M.E., Duarte, A.G., and Way, D.A.: Plant carbon metabolism and climate change:
- 1058 elevated CO<sub>2</sub> and temperature impacts on photosynthesis, photorespiration and respiration, New Phytologist, 221, 32-49, https://doi.org/10.1111/nph.15283, 2019. 1059
- Dyke, A. S. and Prest, V. K.: Late Wisconsinan and Holocene history of the Laurentide Ice 1060
- 1061 Sheet, Géogr. Phys. Quat., 41, 237-263, https://doi.org/10.7202/032681ar, 1987.
- 1062 Edwards, E.J., Osborne, C.P., Strömberg, C.A., Smith, S.A. and C4 Grasses Consortium: The
- 1063 origins of C4 grasslands: integrating evolutionary and ecosystem science, Science, 328,
- 1064 587-591, https://doi.org/10.1126/science.1177216, 2010.
- 1065 Ehleringer, J.R., Cerling, T.E., and Helliker, B.R.: C4 photosynthesis, atmospheric CO<sub>2</sub>, and climate, Oecologia, 112, 285-299, 1997.
- 1066 1067 Faegri, K., Kaland, P.E. and Krzywinski, K., Textbook of pollen analysis, 4<sup>th</sup>Edition, John Wiley
- & Sons Ltd., Chichester, 1989. 1068
- 1069 Dioxide between Terrestrial Plants and the Atmosphere, in: Stable Isotopes and Plant 1070

Farquhar, G.D. and Lloyd, J.: Carbon and Oxygen Isotope Effects in the Exchange of Carbon

- 1071 Carbon/Water Relations, edited by: Ehleringer, J.R., Hall, A.E., and Farguhar, G.D.,
- 1072 Academic Press, New York, 47-70, https://doi.org/10.1016/C2009-0-03312-1,1993.
- 1073 Fletcher, W.J. and Sánchez Goñi, M.F.: Orbital-and sub-orbital-scale climate impacts on
- 1074 vegetation of the western Mediterranean basin over the last 48,000 yr, Quaternary Res.,
- 70, 451-464, https://doi.org/10.1016/j.yqres.2008.07.002, 2008. 1075

- Fletcher, W.J., Goñi, M.S., Peyron, O., and Dormoy, I.: Abrupt climate changes of the last deglaciation detected in a Western Mediterranean forest record, Clim. Past, 6, 245-264, https://doi.org/10.5194/cp-6-245-2010, 2010a.
- Fletcher, W.J., Sánchez Goñi, M.F., Allen, J.R.M., Cheddadi, R., Combourieu-Nebout, N., 1079 1080 Huntley, B., Lawson, I., Londeix, L., Magri, D., Margari, V., Müller, U.C., Naughton, F., Novenko, E., Roucoux, K., Tzedakis, P.C.: Millennial-scale variability during the last glacial 1081 vegetation records from Europe, 2839-2864, 1082 Quat. 29, 1083 https://doi.org/10.1016/j.quascirev.2009.11.015, 2010b.
- García-Ruiz, J. M., Palacios, D., González-Sampériz, P., De Andrés, N., Moreno, A., Valero-Garcés, B., and Gómez-Villar, A.: Mountain glacier evolution in the Iberian Peninsula during the Younger Dryas, Quat. Sci. Rev., 138, 16–30, https://doi.org/10.1016/j.quascirev.2016.02.012, 2016.
- Georget, M., Castéra, M.-H., Devaux, L., Turon, J.-L., Desprat, S., and Sánchez Goñi, M. F.:
  Protocol for pollen and dinocyst analysis in marine sediments, Protocols.io, https://doi.org/10.17504/protocols.io.x54v92qz4l3e/v1, 2025.
- 1091 Gerhart, L.M. and Ward, J.K.: Plant responses to low [CO<sub>2</sub>] of the past, New Phytol., 188, 674-1092 695, https://doi.org/10.1111/j.1469-8137.2010.03441.x, 2010.
- Gomes, S.D., Fletcher, W.J., Rodrigues, T., Stone, A., Abrantes, F., and Naughton, F.: Timetransgressive Holocene maximum of temperate and Mediterranean forest development across the Iberian Peninsula reflects orbital forcing, Palaeogeogr. Palaeocl., 550, 109739, https://doi.org/10.1016/j.palaeo.2020.109739, 2020.
- Gosling, William D., Charlotte S. Miller, Timothy M. Shanahan, Philip B. Holden, Jonathan T. Overpeck, and Frank van Langevelde: A Stronger Role for Long-Term Moisture Change Than for CO<sub>2</sub> in Determining Tropical Woody Vegetation Change. Science 376 (6593): 653–56. https://doi.org/10.1126/science.abg4618, 2022.
- Gratani, L. and Varone, L.: Leaf key traits of Erica arborea L., Erica multiflora L. and Rosmarinus officinalis L. co-occurring in the Mediterranean maquis. Flora-Morphology, Distribution, Functional Ecology of Plants, 199, 58-69, https://doi.org/10.1078/0367-2530-00130, 2004.
- Grimalt, J. O., Calvo, E., and Pelejero, C.: Sea surface paleotemperature errors in U<sup>k</sup>'37 estimation due to alkenone measurements near the limit of detection, Paleoceanography, 16, 226-232, 10.1029/1999PA000440, 2001.
- Grimm, E. C.: CONISS: a FORTRAN 77 program for stratigraphically constrained cluster analysis by the method of incremental sum of squares, Comput. Geosci., 13, 13–35, https://doi.org/10.1016/0098-3004(87)90022-7, 1987.
- Guiot, J., Torre, F., Jolly, D., Peyron, O., Boreux, J.J., and Cheddadi, R.: Inverse vegetation modeling by Monte Carlo sampling to reconstruct palaeoclimates under changed precipitation seasonality and CO2 conditions: application to glacial climate in Mediterranean region, Ecol. Model., 127, 119-140, https://doi.org/10.1016/S0304-3800(99)00219-7, 2000.
- Harrison, S.P. and Prentice, C.I.: Climate and CO<sub>2</sub> controls on global vegetation distribution at the last glacial maximum: analysis based on palaeovegetation data, biome modelling and palaeoclimate simulations, Glob. Chang. Biol., 9, 983-1004, https://doi.org/10.1046/j.1365-2486.2003.00640.x, 2003.
- Heaton, T.J., Köhler, P., Butzin, M., Bard, E., Reimer, R.W., Austin, W.E., Ramsey, C.B, Grootes, P.M., Hughen, K.A, Kromer, B., Reimer, P.J., Adkins, J., Burke, A., Cook, M.S.,
- Olsen, J., Skinner, L.C. :Marine20—the marine radiocarbon age calibration curve (0-
- 55,000 cal BP), Radiocarbon,62(4), 779-820, https://doi.org/10.1017/RDC.2020.68, 2020.

- Heusser, L. and Balsam, WL: Pollen distribution in the northeast Pacific Ocean, Quaternary Res., 7, 45-62, https://doi.org/10.1016/0033-5894(77)90013-8, 1977.
- Hodell, D., Lourens, L., Crowhurst, S., Konijnendijk, T., Tjallingii, R., Jiménez-Espejo, F., Skinner, L., Tzedakis, P.C., Members, T.S.S.P., Abrantes, F., and Acton, G.D.: A reference time scale for Site U1385 (Shackleton Site) on the SW Iberian Margin, Global and Planet. Change, 133, 49-64, https://doi.org/10.1016/j.gloplacha.2015.07.002, 2015.
- Huang, J.G., Bergeron, Y., Denneler, B., Berninger, F., and Tardif, J.: Response of forest trees to increased atmospheric CO<sub>2</sub>, Critical Reviews in Plant Sciences, 26, 265-283, 2007.
- 1132 Izumi, K. and Lézine, A.M.: Pollen-based biome reconstructions over the past 18,000 years 1133 and atmospheric CO<sub>2</sub> impacts on vegetation in equatorial mountains of Africa, Quat. Sci. 1134 Rev., 152, 93-103, https://dx.doi.org/10.1016/j.quascirev.2016.09.023, 2016.
- Izumi, K., and Bartlein, P. J.: North American paleoclimate reconstructions for the Last Glacial Maximum using an inverse modeling through iterative forward modeling approach applied to pollen data. Geophys. Res. Lett, 43(20), 10-965, https://doi.org/10.1002/2016GL070152, 2016.
- Jetter, R., Kunst, L., and Samuels, A.L.: Composition of plant cuticular waxes, in: Biology of the Plant Cuticle, Annual Plant Reviews, edited by: Riederer, M., Müller, C., Blackwell, Oxford, 145-181, https://doi.org/10.1002/9780470988718.ch4, 2006.
- Jolly, D. and Haxeltine, A.: Effect of Low Glacial Atmospheric CO<sub>2</sub> on Tropical African Montane Vegetation, Science, 276, 786-788, https://doi.org/10.1126/SCIENCE.276.5313.786, 1997.
- 1144 Körner, C.: Biosphere responses to CO<sub>2</sub> enrichment, Ecol. Appl., 10, 1590-1145 1619,https://doi.org/10.1890/1051-0761(2000)010[1590: BRTCE]2.0.CO;2, 2000.
- Ludwig, P., Shao, Y., Kehl, M., and Weniger, G.-C.: The Last Glacial Maximum and Heinrich event I on the Iberian Peninsula: A regional climate modelling study for understanding human settlement patterns, Glob. Planet. Change, 170, 34-47, https://doi.org/10.1016/J.GLOPLACHA.2018.08.006, 2018.
- Koutsodendris, A., Dakos, V., Fletcher, W. J., Knipping, M., Kotthoff, U., Milner, A. M., Müller, U. C., Kaboth-Bahr, S., Kern, O. A., Kolb, L., Vakhrameeva, P., Wulf, S., Christanis, K., Schmiedl, G., and Pross, J.: Atmospheric CO<sub>2</sub> forcing on Mediterranean biomes during the past 500 kyrs, Nat. Commun. 14, 1664, https://doi.org/10.1038/s41467-023-37388-x, 2023.
- Marcott, S.A., Bauska, T.K., Buizert, C., Steig, E.J., Rosen, J.L., Cuffey, K.M., Fudge, T.J., Severinghaus, J.P., Ahn, J., Kalk, M.L., McConnell, J.R., Sowers, T., Taylor, K.C., White, J.W.C., Brook, E.J.: Centennial-scale changes in the global carbon cycle during the last deglaciation, Nature, 514, 616-619, https://doi.org/10.1038/nature13799, 2014.
- Margari, V., Skinner, L.C., Hodell, D.A., Martrat, B., Toucanne, S., Grimalt, J.O., Gibbard, P.L., Lunkka, J.P. and Tzedakis, P.C.: Land-ocean changes on orbital and millennial time scales and the penultimate glaciation. Geology, 42(3), pp.183-186, https://doi.org/10.1130/G35070.1, 2014.
- Martrat, B., Grimalt, J. O., Shackleton, N. J., de Abreu, L., Hutterli, M. A., and. Stocker, T. F.:
  Four climate cycles of recurring deep and surface water destabilisations on the Iberian margin, Science, 317, 502 507, https://doi.org/10.1126/science.1139994, 2007.
- McAndrews, J.H. and King, J.E.: Pollen of the North American Quaternary: the top twenty, Geoscience and Man, 15, 41-49, https://doi.org/10.2307/3687256, 1976.
- Meijer, P. T. and Tuenter, E.: The effect of precession-induced changes in the Mediterranean freshwater budget on circulation at shallow and intermediate depth, Journal of Marine Systems, 68, 349–365, https://doi.org/10.1016/j.jmarsys.2007.01.006, 2007.

- Meyers, P.A.: Applications of organic geochemistry to paleolimnological reconstructions: a summary of examples from the Laurentian Great Lakes, Org. Geochem., 34, 261-289,
- https://doi.org/10.1016/S0146-6380(02)00168-7, 2003.
- Monnin, E., Indermühle, A., Dällenbach, A., Flückiger, J., Stauffer, B., Stocker, T.F., Raynaud,
- D., Barnola, J.M.: Atmospheric CO2 concentrations over the last glacial termination, Science, 291, 112-114, https://doi.org/10.1126/science.291.5501.112, 2001.
- Moore, P.D., Webb, J.A. and Collison, M.E.: Pollen analysis. Blackwell scientific publications, Oxford, 1991.
- Morales-Molino, C. and García-Antón, M.: Vegetation and fire history since the last glacial maximum in an inland area of the western Mediterranean Basin (Northern Iberian Plateau, NW Spain), Quaternary Res., 81, 63-77, https://doi.org/10.1016/j.yqres.2013.10.010, 2014.
- Morales-Molino, C., Devaux, L., Georget, M., Hanquiez, V., and Goñi, M.F.S.: Modern pollen representation of the vegetation of the Tagus Basin (central Iberian Peninsula), Rev. Palaeobot. Palyno., 276, 104193, https://doi.org/10.1016/j.revpalbo.2020.104193, 2020.
- Müller, P., Kirst, G., Ruhland, G., Storch, I.V., Rosell-Melé, A.: Calibration of the alkenone index U<sup>k</sup><sub>37</sub> based on core-tops the eastern South Atlantic and global ocean (60°N-60°S), Geochim. Cosmochim. Ac., 62, 1757-1772, https://doi.org/10.1016/S0016-7037(98)00097-0, 1998.
- Naughton, F., Costas, S., Gomes, S.D., Desprat, S., Rodrigues, T., Goñi, M.S., Renssen, H., Trigo, R., Bronk-Ramsey, C., Oliveira, D., and Salgueiro, E.: Coupled ocean and atmospheric changes during Greenland stadial 1 in southwestern Europe, Quaternary Sci. Rev., 212, 108-120, https://doi.org/10.1016/j.quascirev.2019.03.033, 2019.
- Naughton, F., Drago, T., Sánchez-Goñi, M.F., and Freitas, M.C.: Climate variability in the North-Western Iberian Peninsula during the last deglaciation, in: Oceans and the atmospheric carbon content, edited by: Duarte, P., Santana-Casiano, M., Springer, Dordrecht, 1-22, 2011.
- Naughton, F.,Sanchéz-Goñi, M.S., Desprat, S., Turon, J.L., Duprat, J., Malaizé, B., Joli, C., Cortijo, E., Drago, T., and Freitas, M.C.: Present-day and past (last 25 000 years) marine pollen signal off western Iberia, Marine Micropaleontology, 62, 91-114, 10.1016/j.marmicro.2006.07.006, 2007.
- Naughton, F., Sánchez Goñi, M.S., Rodrigues, T., Salgueiro, E., Costas, S., Desprat, S., Duprat, J., Michel, E., Rossignol, L., Zaragosi, S., and Voelker, A.H.L.: Climate variability across the last deglaciation in NW Iberia and its margin, Quaternary Int., 414, 9-22, https://doi.org/10.1016/j.quaint.2015.08.073, 2016.
- Nelson, D.M., Urban, M.A., Kershaw, A.P., and Hu, F.S.: Late-Quaternary variation in C3 and C4 grass abundance in southeastern Australia as inferred from δ13C analysis: Assessing the roles of climate, pCO2, and fire, Quaternary Sci. Rev., 139, 67-76, https://doi.org/10.1016/j.quascirev.2016.03.006, 2016.
- Oliveira, D., Desprat, S., Rodrigues, T., Naughton, F., Hodell, D., Trigo, R., Rufino, M., Lopes, 1208 C., Abrantes, F., and Sánchez Goñi, M. F.: The complexity of millennial-scale variability in 1209 1210 southwestern Europe during MIS 11, Quat. Res., 86. 373–387. 1211 https://doi.org/10.1016/j.ygres.2016.09.002, 2016.
- Oliveira, D., Desprat, S., Yin, Q., Naughton, F., Trigo, R., Rodrigues, T., Abrantes, F., and Sánchez Goñi, M.F.: Unraveling the forcings controlling the vegetation and climate of the best orbital analogues for the present interglacial in SW Europe, Clim. Dynam., 51, 667-686, https://doi.org/10.1007/s00382-017-3948-7, 2018.
- Oliveira, D., Desprat, S., Yin, Q., Rodrigues, T., Naughton, F., Trigo, R. M., and Goñi, M. F. S. Combination of insolation and ice-sheet forcing drive enhanced humidity in northern

- subtropical regions during MIS 13. Quat. Sci. Rev., 247, 106573, https://doi.org/10.1016/j.quascirev.2020.106573, 2020.
- Ortiz, J.E., Torres, T., Delgado, A., Llamas, J.F., Soler, V., Valle, M., Julià, R., Moreno, L., and Díaz-Bautista, A.: Palaeoenvironmental changes in the Padul Basin (Granada, Spain) over the last 1 Ma based on the biomarker content, Palaeogeogr. Palaeocl., 298, 286-299, https://doi.org/10.1016/j.palaeo.2010.10.003, 2010.
- Pausas, J.G., Llovet, J., Rodrigo, A., and Vallejo, R.: Are wildfires a disaster in the Mediterranean basin? A review, Int. J. Wildland Fire , 17, 713-723, https://doi.org/10.1071/WF07151, 2008.
- Pearson, P.N. and Palmer, M.R.: Atmospheric carbon dioxide concentrations over the past 60 million years, Nature, 406, 695-699, https://doi.org/10.1038/35021000, 2000.
- Peñalba, M.C., Arnold, M., Guiot, J., Duplessy, J.C., Beaulieu, J.-L.: Termination of the last glaciation in the Iberian Peninsula inferred from the pollen sequence of Quintanar de la Sierra, Quaternary Res., 48, 205-214, https://doi.org/10.1006/qres.1997.1922,1997.
- Pèrez-Obiol, R. and Julià, R.: Climatic change on the Iberian Peninsula recorded in a 30,000yr pollen record from Lake Banyoles, Quaternary Res., 41, 91-98, https://doi.org/10.1006/qres.1994.1010, 1994.
- Peyron, O., Guiot, J., Cheddadi, R., Tarasov, P., Reille, M., de Beaulieu, J.L., Bottema, S., and Andrieu, V.: Climatic reconstruction in Europe for 18,000 yr BP from pollen data, Quaternary Res., 49, 183-196,https://doi.org/10.1006/qres.1997.1961,1998.
- Piao S, Wang X, Park T, Chen C, Lian XU, He Y, Bjerke JW, Chen A, Ciais P, Tømmervik H, Nemani RR: Characteristics, drivers and feedbacks of global greening. Nat. Rev. Earth Environ., 1(1), 14–27. https://doi.org/10.1038/s43017-019-0001-x, 2020.
- Post-Beittenmiller, D.: Biochemistry and molecular biology of wax production in plants, Annu. Rev. Plant Biol., 47, 405-430, https://doi.org/10.1146/annurev.arplant.47.1.405, 1996.
- Prahl, F.G. and Wakeham, S.G.: Calibration of unsaturation patterns in long-chain ketone compositions for palaeotemperature assessment, Nature, 330, 367-369, https://doi.org/10.1038/330367a0, 1987.
- Prentice, I.C., Cleator, S.F., Huang, Y.H., Harrison, S.P., and Roulstone, I.: Reconstructing ice-age palaeoclimates: Quantifying low-CO2 effects on plants, Glob. Planet. Change, 149, 166-176, https://doi.org/10.1016/J.GLOPLACHA.2016.12.012, 2017.
- Prentice, I. C., Villegas-Diaz, R., and Harrison, S. P.: <u>Accounting Account ing</u> for atmospheric carbon dioxide variations in pollen-based reconstruction of past hydroclimates, Global Planet. Change, 211, 103790, https://doi.org/10.1016/j.gloplacha.2022.103790, 2022.
- R Development Core Team R: A Language and Environment for Statistical Computing. R Foundation for Statistical Computing, Vienna, Austria, https://www.R-project.org/, 2020.
- Reille, M.: Pollen et spores d'Europe et d'Afrique du nord: Laboratoire de botanique historique et palynologie, URA CNRS, Marseille, France, 543p., 1992.
- Reille, M.: Pollen et spores d'Europe et d'Afrique du Nord (Vol. 2), Laboratoire de Botanique historique et Palynologie, URA CNRS, Marseille, France, 1995.
- Rivas-Martínez, S., Penas, Á., del Río, S., Díaz González, T.E., and Rivas-Sáenz, S.: Bioclimatology of the Iberian Peninsula and the Balearic Islands, in The Vegetation of the Iberian Peninsula, edited by: Loidi, J., Plant and Vegetation, vol. 12, Springer, Cham, Switzerland, pp. 29–80, https://doi.org/10.1007/978-3-319-54784-8 2, 2017.
- Rodrigues, T., Alonso-García, M., Hodell, D.A., Rufino, M., Naughton, F., Grimalt, J.O., Voelker, A.H.L., and Abrantes, F.: A 1-Ma record of sea surface temperature and extreme
- cooling events in the North Atlantic: A perspective from the Iberian Margin, Quaternary Sci.
- 1265 Rev., 172, 118-130, https://doi.org/10.1016/j.quascirev.2017.07.004, 2017.

- Rodrigues, T., Grimalt, J.O., Abrantes, F., Naughton, F., and Flores, J.A.: The last glacial-interglacial transition (LGIT) in the western mid-latitudes of the North Atlantic: Abrupt sea surface temperature change and sea level implications, Quaternary Sci. Rev., 29, 1853-1862, https://doi.org/10.1016/j.quascirev.2010.04.004, 2010.
- Royer, D. L. Stomatal density and stomatal index as indicators of paleoatmospheric CO<sub>2</sub> concentration. Review of Palaeobotany and Palynology, 114(1-2), 1-28, https://linkinghub.elsevier.com/retrieve/pii/S0034666700000749, 2001.
- Sage, R.F. and Cowling, S.A.: Implications of stress in low CO<sub>2</sub> atmospheres of the past: Are today's plants too conservative for a high CO<sub>2</sub> world?, in: Carbon dioxide and environmental stress, edited by: Luo, Y., Mooney, H.A., Academic Press, New York, 289- 305, https://doi.org/10.1016/B978-012460370-7/50012-7, 1999.
- Shakun, J.D., Clark, P.U., He, F., Marcott, S.A., Mix, A.C., Liu, Z., Otto-Bliesner, B., Schmittner, A., Bard, E.: Global warming preceded by increasing carbon dioxide concentrations during the last deglaciation, Nature, 484, 49-54, https://doi.org/10.1038/nature10915, 2012.
- Shao, Y., Anhäuser, A., Ludwig, P., Schlüter, P., and Williams, E.: Statistical reconstruction of global vegetation for the last glacial maximum, Glob. Planet. Change, 168, 67-77, https://doi.org/10.1016/j.gloplacha.2018.06.002, 2018.
- Simpson, G.L.: Modelling palaeoecological time series using generalised additive models, Front. Eco. Evo., 6, 149, https://doi.org/10.3389/fevo.2018.00149, 2018.
- Stockmarr, J.A.: Tablets with spores used in absolute pollen analysis, Pollen spores, 13, 615-621, 1971.
- Street-Perrott, F.A., Huang, Y., Perrott, A., Eglinton, G., Barker, P., Khelifa, L.B, Harkness, D.D., Olago, D.O.: Impact of lower atmospheric carbon dioxide on tropical mountain ecosystems, Science, 278, 1422-1426, https://doi.org/10.1126/science.278.5342.1422, 1997.
- Struck, J., Bliedtner, M., Strobel, P., Schumacher, J., Bazarradnaa, E., and Zech, R.: Leaf wax n-alkane patterns and compound-specific δ<sup>13</sup>C of plants and topsoils from semi-arid and arid Mongolia, Biogeosciences, 17, 567–580, https://doi.org/10.5194/bg-17-567-2020, 2020.
- Svenning, J.C., Fløjgaard, C., Marske, K.A., Nógues-Bravo, D., and Normand, S.: Applications of species distribution modelling to paleobiology, Quaternary Sci. Rev., 30, 2930-2947, https://doi.org/10.1016/j.quascirev.2011.06.012, 2011.
- Tarroso, P., Carrión, J., Dorado-Valiño, M., Queiroz, P., Santos, L., Valdeolmillos-Rodríguez, A., Célio Alves, P., Brito, J.C., and Cheddadi, R.: Spatial Climate Dynamics in the Iberian Peninsula since 15 000 yr BP, Clim. Past, 12, 1137-1149, https://doi.org/10.5194/cp-12-1302 1137-2016, 2016.
- Tognetti, R., Cherubini, P., and Innes, J.L.: Comparative stem-growth rates of Mediterranean trees under background and naturally enhanced ambient CO<sub>2</sub> concentrations, New Phytol., 146, 59-74, https://doi.org/10.1046/j.1469-8137.2000.00620.x, 2008.
- Toucanne, S., Zaragosi, S., Bourillet, J. F., Naughton, F., Cremer, M., Eynaud, F., and Dennielou, B.: Activity of the turbidite levees of the Celtic–Armorican margin (Bay of Biscay) during the last 30 000 years: imprints of the last European deglaciation and Heinrich events.
- 1309 Mar. Geol., 247, 84–103, https://doi.org/10.1016/j.margeo.2007.08.006, 2008.Tripati, A.K.,
- Roberts, C.D., and Eagle, R. A.: Coupling of CO<sub>2</sub> and Ice Sheet Stability Over Major Climate
- 1311 Transitions of the Last 20 Million Years, Science, 326, 1394-1397.
- 1312 https://doi.org/10.1126/science.1178296, 2009.
- 1313 Turon, J.L., Lézine, A.M., and Denèfle, M.: Land-sea correlations for the last glaciation inferred

- from a pollen and dinocyst record from the Portuguese margin, Quaternary Res., 59, 88-96, https://doi.org/10.1016/S0033-5894(02)00018-2, 2003.
- Villanueva, J. and Grimalt, J.O.: Gas Chromatographic Tuning of the U<sup>k</sup>'<sub>37</sub> Paleothermometer, Anal. Chem., 69, 3329-3332, https://doi.org/10.1021/ac9700383, 1997.
- Volkman, J.K., Barrerr, SM, Blackburn, S.I. and Sikes, E.L.: Alkenones in Gephyrocapsa oceanica: Implications for studies of paleoclimate, Geochim. Cosmochim. Ac., 59, 513-520, https://doi.org/10.1016/0016-7037(95)00325-T, 1995.
- Wagner F., Below R., de Klerk P., Dilcher D.L., Joosten H., Kürschner W.M. and Visscher H.:

   A natural experiment on plant acclimation: lifetime stomatal frequency response of an individual tree to annual atmospheric CO<sub>2</sub> increase. Proc. Natl. Acad. Sci. U.S.A., 93(21), 11705–11708, https://doi.org/10.1073/pnas.93.21.11705, 1997.
- Ward, J.K.: Evolution and growth of plants in a low CO<sub>2</sub> world, in: A history of atmospheric CO<sub>2</sub> and its effects on plants, animals, and ecosystems, edited by: Ehleringer, J.R., Cerling, T.E., Dearing, M.D., Springer, New York, 232-257, 2005.
- Wei, D., González-Sampériz, P., Gil-Romera, G., Harrison, S. P., and Prentice, I. C.: Seasonal temperature and mois ture changes in interior semi-arid Spain from the last inter glacial to the Late Holocene, Quaternary Res., 101, 143–155, https://doi.org/10.1017/qua.2020.108, 2021.
- Woillez, M., Kageyama, M., Krinner, G., de Noblet-Ducoudré, N., Viovy, N., and Mancip, M.: Impact of CO<sub>2</sub> and climate on the Last Glacial Maximum vegetation: results from the ORCHIDEE/IPSL models, Clim. Past, 7, 557-577, https://doi.org/10.5194/cp-7-557-2011, 2011.
- Wood, S. N.: Generalised Additive Models: An Introduction with R, 2<sup>nd</sup> Edition, Chapman and Hall/CRC Press, New York, 496p., https://doi.org/10.1201/9781315370279, 2017.
- Wu, H., Guiot, J., Brewer, S., and Guo, Z.: Climatic changes in Eurasia and Africa at the last glacial maximum and mid-Holocene: reconstruction from pollen data using inverse vegetation modelling, Clim. Dyn., 29, 211-229, https://doi.org/10.1007/s00382-007-0231-3, 2007.

1343

1344

1345

1346

1347

1348

1349

1350

1351

1352

# 1354 Tables and figures

# **Table 1 – AMS R**radiocarbon ages of IODP Site U1385.

| Core<br>Depth (crmcd) | Material   | Conv.         | Error         |  |
|-----------------------|--|---------------|---------------|--|
|                       |  | (yr B.P.)     |               |  |
| 52                    | G. bulloides   | 2525          | 28            |  |
|                       |  |               |               |  |
| 108                   | G. bulloides   | 6181          | 35            |  |
| 156                   | G. bulloides   | 10060         | 33            |  |
|                       |  |               |               |  |
| 186                   | G. bulloides   | 11310         | 60            |  |
|                       |  |               |               |  |
| 193                   | G. bulloides   | 11499         | 43            |  |
| 217                   | G. bulloides   | 12300         | 40            |  |
|                       |  |               |               |  |
| 237                   | G. bulloides   | 13430         | 110           |  |
| 248                   | G hulloides  | 13355         | 45            |  |
| 210                   | o. bandaco   | 10000         | 10            |  |
| 251                   | G. bulloides   | 13670         | 60            |  |
|                       |  |               |               |  |
| 303                   | G. bulloides   | 15890         | 70            |  |
| 333                   | G. bulloides   | 17090         | 90            |  |
|                       |  |               |               |  |
| 363                   | G. bulloides   | 18010         | 60            |  |
| 200                   | G. inflata   | 40700         | 70            |  |
| UCIAMS-235001 390     |  | 18700         | 70            |  |
| 431                   | G. bulloides   | 19540         | 70            |  |
|                       | G. inflata   |               |               |  |
| UCIAMS-235003 447     | G. bulloides   | 20910         | 90            |  |
| 427                   |  | 24020         | 100           |  |
| 40/                   | G. bulloides G. inflata                                | Z103U         | 100           |  |
|                       | 52 108 156 186 187 217 237 248 251 303 333 363 390 431 | Depth (crmcd) | Depth (crmod) | Depth (crmod)  AMS <sup>14</sup> C (yr B.P.)  52 |

<sup>\*</sup> AMS from Oliveira et al. (2018)

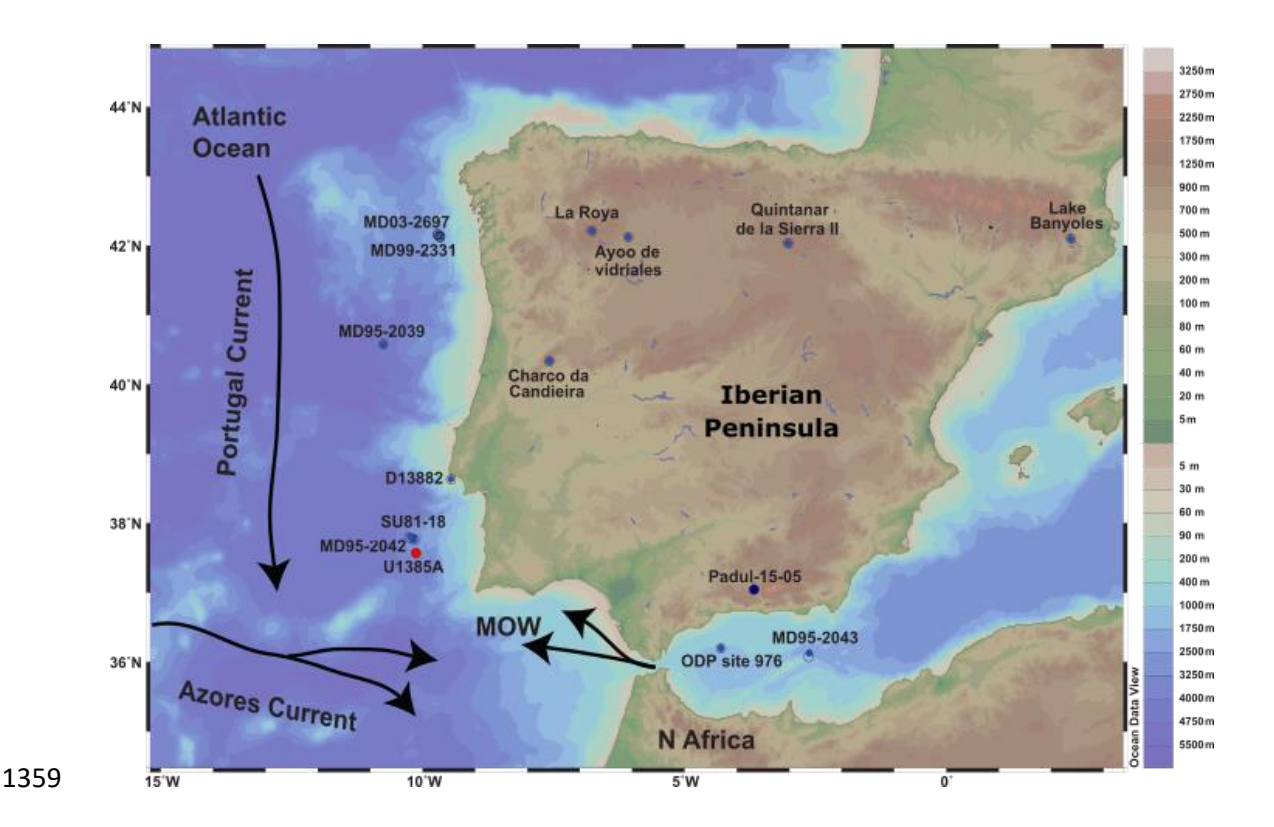
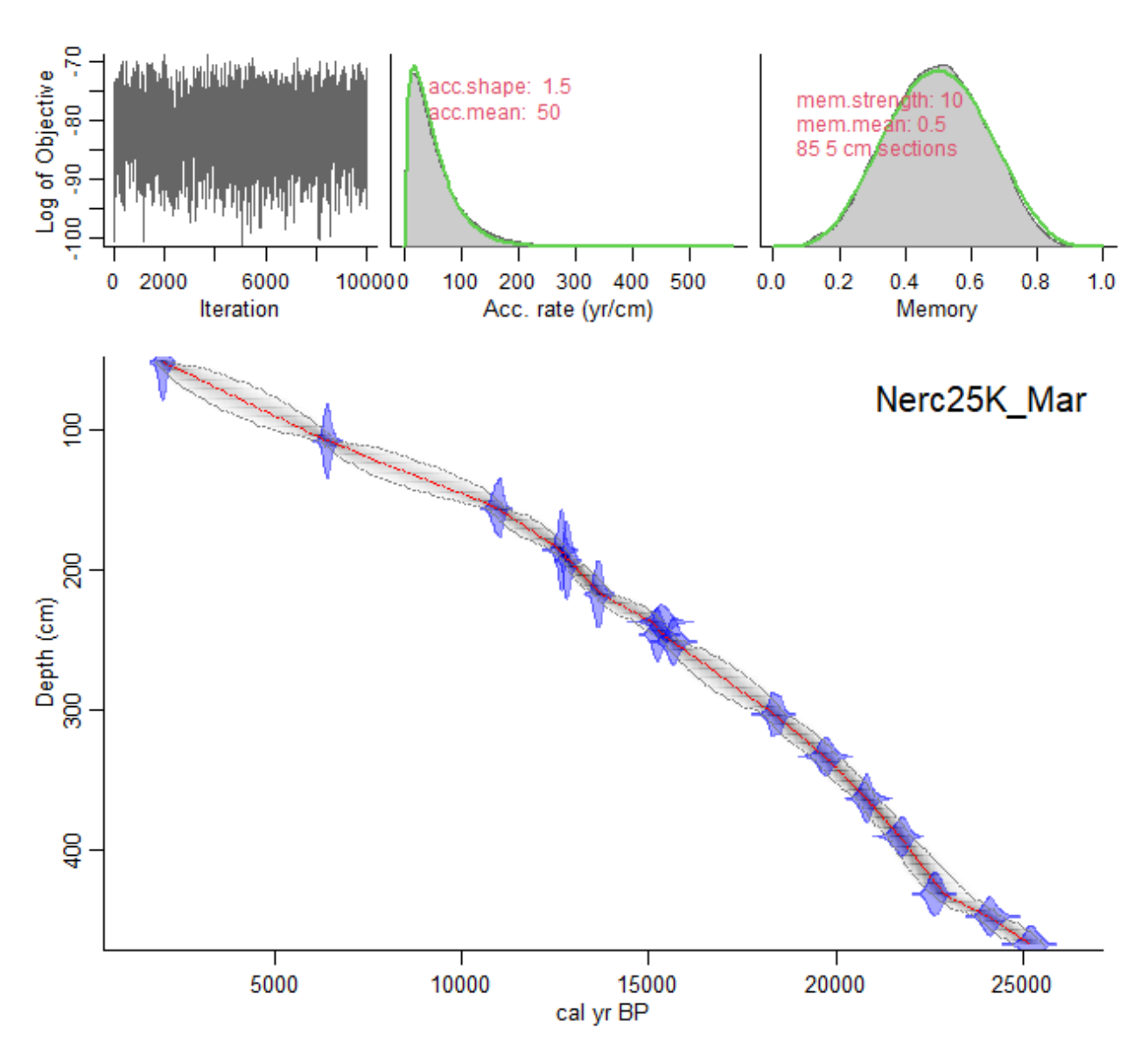
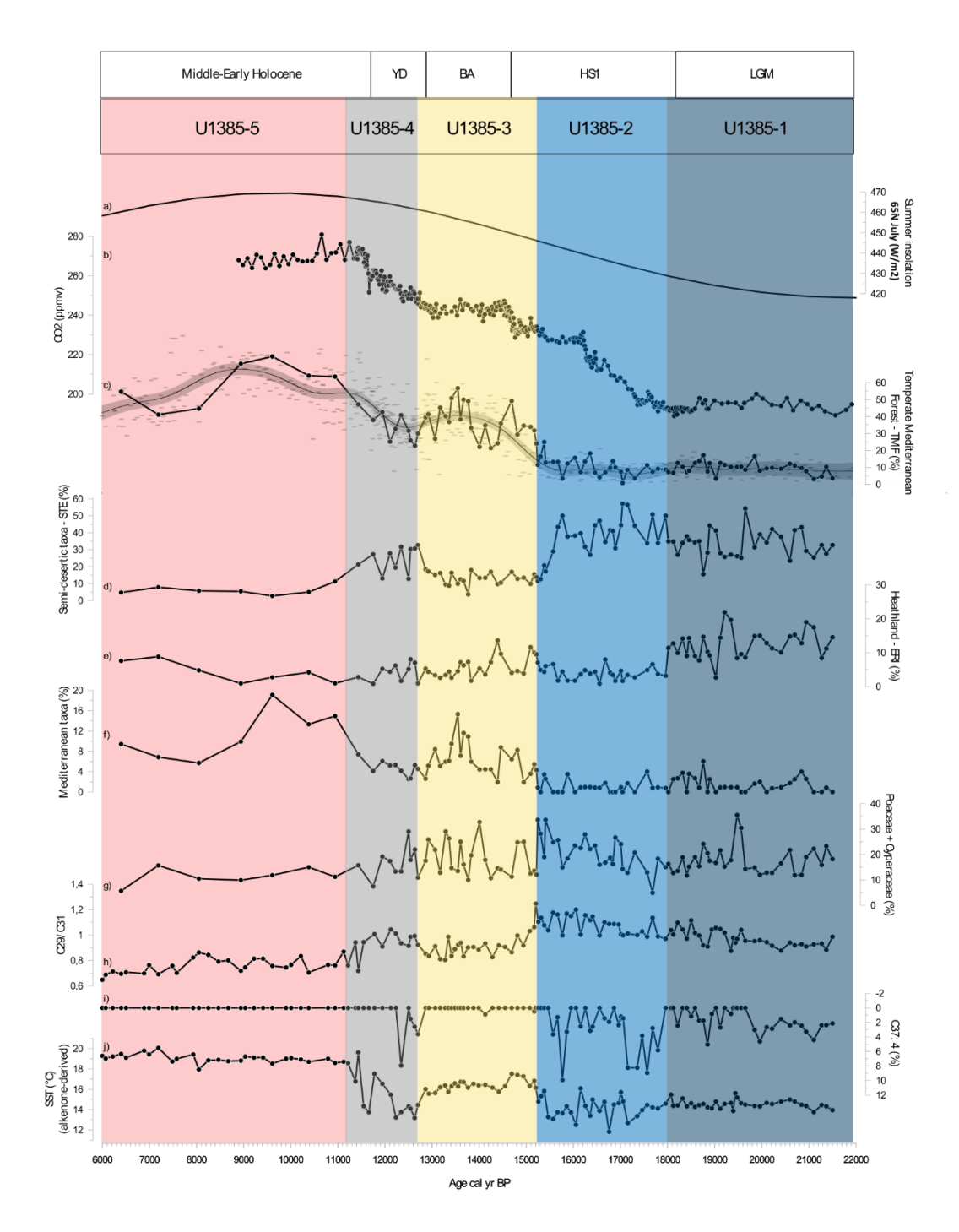


Figure 1 – Location of the IODP Site U1385 and of the marine and terrestrial pollen records discussed in the text. Marine sedimentary records: MD03-2697 (Naughton et al., 2016); MD99-2331 (Naughton et al., 2007); MD95-2039 (Roucoux et al., 2005); D13882 (Gomes et al., 2020); MD95-2043 (Fletcher and Sánchez Goñi, 2008); MD95-2042 (Chabaud et al., 2014); SU81-18 (Turon et al., 2003); ODP Site 976 (Combourieu Comborieut Nebout et al., 1998; 2002; 2009); Continental sedimentary records: Lake de Banyoles (Pèrez-Obiol and Julià,1994); Quintanar de la Sierra II (Peñalba et al., 1997); La Roya (Allen et al., 1996); Ayoo de vidriales (Morales-Molino and Garcia-Anton, 2014); Charco da Candieira (Van der Knaap and van Leeuwen, 1997); Padul\_15-05 (Camuera et al., 2019). Black arrows represent the surface water circulation (MOW, Portugal and Azores Current). Note that coastline boundaries are for the present day.



**Figure 2 –** Age-depth model for IODP Site U1385 using a Bayesian approach with Bacon v.2.3.9.1 (Blaauw and Christen, 2011). The original dates were calibrated using Marine20 (Heaton et al., 2020)\_\_g\_Grey stippled lines\_ show 95% confidence intervals; red curve shows single "best" model based on the mean age for each depth. Upper graphs show from left to right: Markov Chain Monte Carlo (MCMC) iterations and priors (green line) and posteriors (dark grey line with a grey fill) for the accumulation rate and variability/memory. Note: the depth (Y axis) was converted to cm from the corrected revised meter composite depth (crmcd).



**Figure 3** – Comparison of multiproxy records from the Site U1385 with a) 65°N July (W/m²) summer insolation (Berger and Loutre, 1991) b) CO2 (ppmv) composite from WAIS (Marcott et al., 2014). — (; Percentages of the Pprincipal pollen-based ecological groups: c) Temperate Mediterranean Forest from Site U1385 (%) (solid black line) and compilation of Iberian Margin TMF records (D13882, MD03-2697; MD95-2042; MD95-2043; ODP-976; U1385) — GAM (curve with grey (%), d) Semi-desertic taxa\_including Amaranthaceae (previously Chenopodiaceae), Artemisia, and Ephedra. (%), e) Heathland\_including members of the Ericaceae family (including various Erica spp) and Calluna spp (%), f) Mediterranean taxa (%) and g) Poaceae + Cyperaceae (%); h) C<sub>29</sub>/C<sub>31</sub> ratio, i) C<sub>37:4</sub> (%) and j) SST (°C). The

1<mark>397</mark>

different coloured shading corresponds to the pollen zones (SM Fig. S1 and SM Table S1) and were connected with the periods indicated.

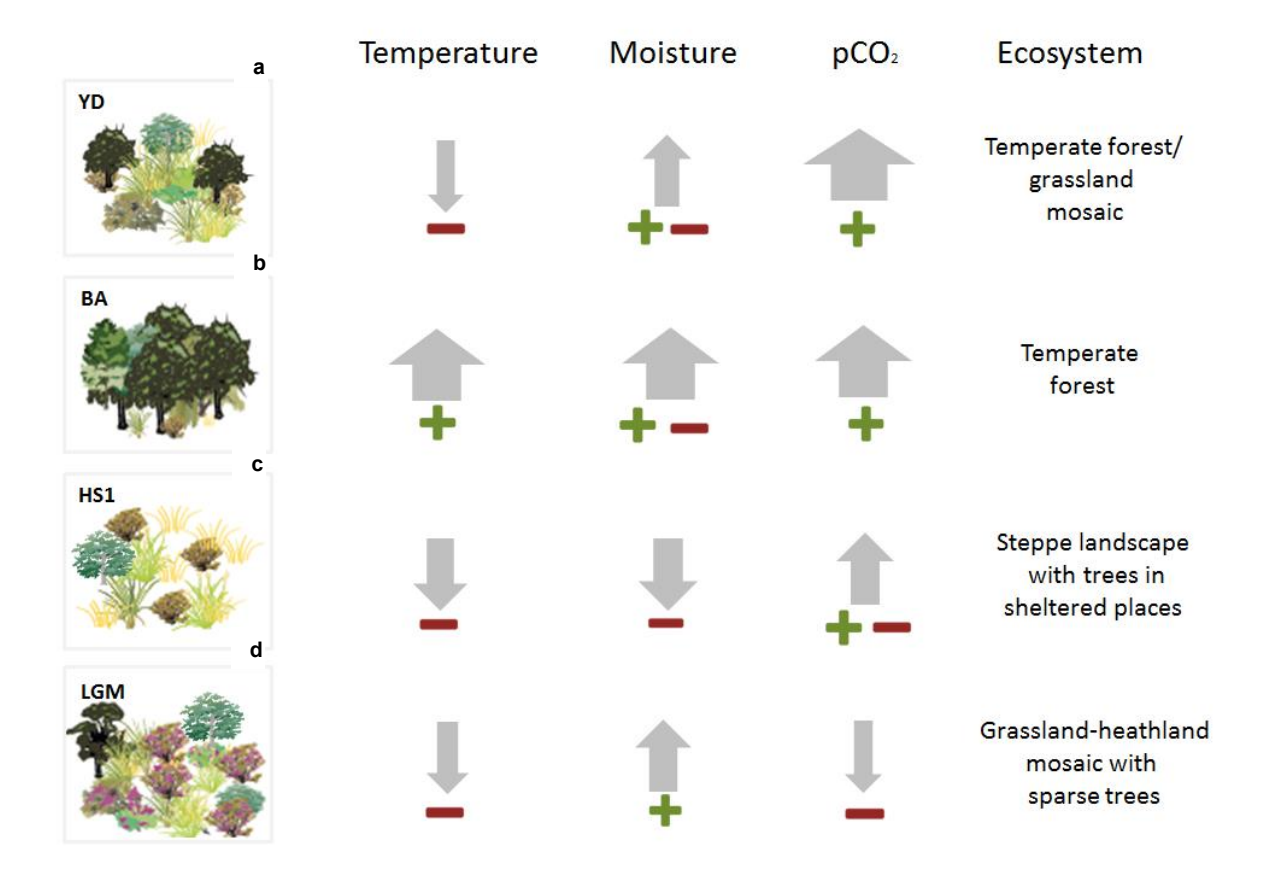


**Figure 4** – Schematic representation of the relative change of climatic inferred parameters (precipitation and temperature) based on pollen- $\frac{\text{vegegation}}{\text{vegegation}}$  groups, biomarkers, SST as well as the physiological contribution of  $CO_2$  for each period showing a schematic reconstruction of the potential ecosystem scenarios. The perceived temperature used the interpretation of pollen (TMF and STE groups), SST and n-alkanes; the perceived moisture (ERI, TMF and STE).

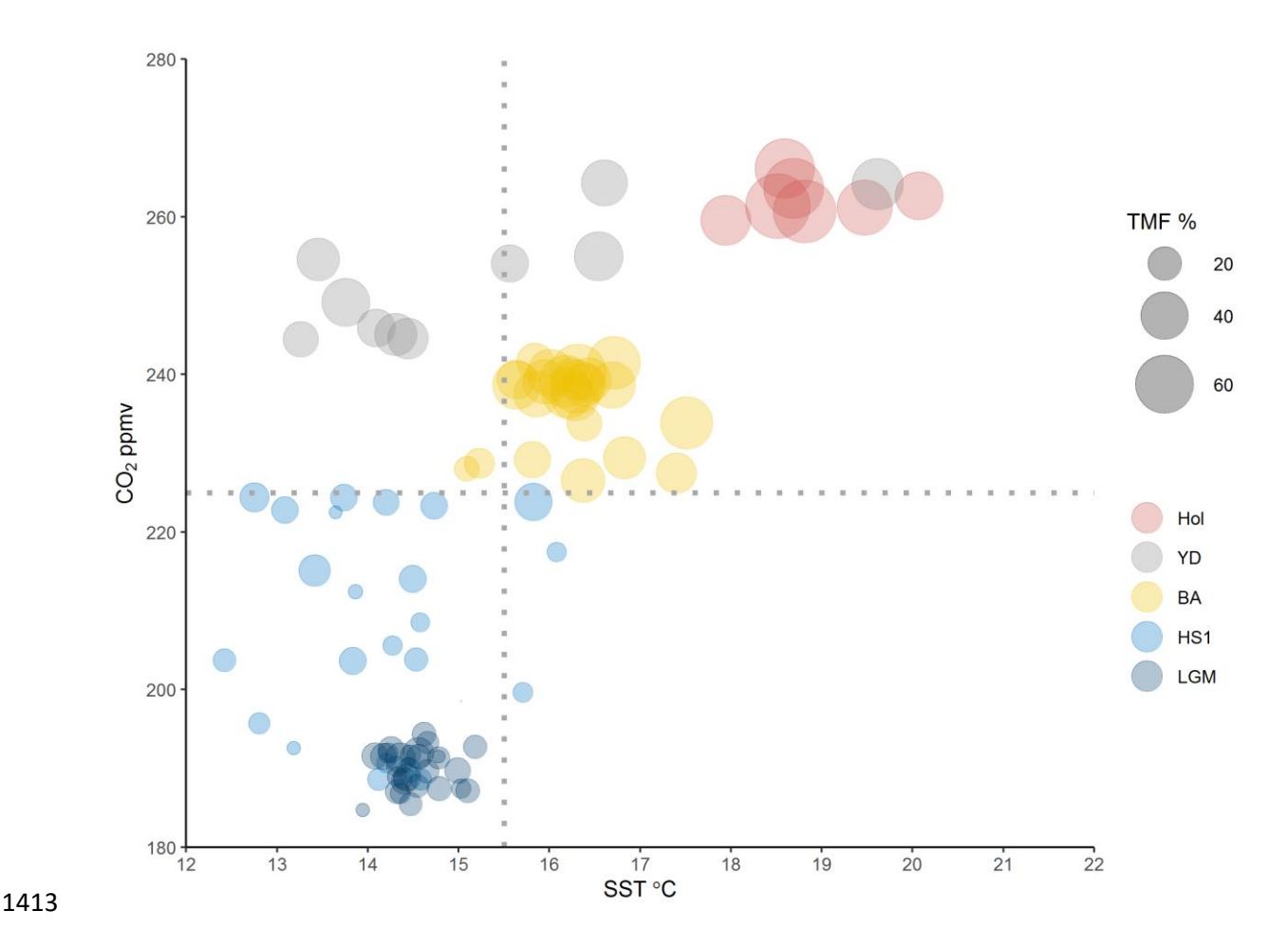


**Figure 5** – Dispersion plot showing the relation between  $CO_2$  (Marcott et al., 2014) and SST in relation to TMF % across the different intervals of the Last deglaciation, following the pollen zones boundaries.